Received: 9 May 2017 | Revised: 30 May 2017 | Accepted: 30 May 2017

DOI: 10.1002/jat.3505

Journal of Applied Toxicology

RESEARCH ARTICLE

Assessment of genotoxicity and biodistribution of nano- and micron-sized yttrium oxide in rats after acute oral treatment

Archana Panyala[1,2] | Srinivas Chinde[1,3] | Srinivas Indu Kumari[1] | Paramjit Grover[1,2]

[1] Toxicology Unit, Pharmacology and Toxicology Division, CSIR – Indian Institute of Chemical Technology, Hyderabad, Telangana 500007, India

[2] Academy of Scientific and Innovative Research, CSIR – Indian Institute of Chemical Technology, Hyderabad, Telangana 500007, India

[3] Department of Genetics, Osmania University, Osmania University Main Road, Hyderabad, Telangana 500007, India

Correspondence
Dr. Paramjit Grover, CSIR-Emeritus Scientist, Toxicology Unit, Pharmacology and Toxicology Division, CSIR – Indian Institute of Chemical Technology, Hyderabad – 500007, Telangana, India.
Email: paramgrover@gmail.com; grover@iict.res.in

Abstract

The increasing use of yttrium oxide (Y_2O_3) nanoparticles (NPs) entails an improved understanding of their potential impact on the environmental and human health. In the present study, the acute oral toxicity of Y_2O_3 NPs and their microparticles (MPs) was carried out in female albino Wistar rats with 250, 500 and 1000 mg kg^{-1} body weight doses. Before the genotoxicity evaluation, characterization of the particles by transmission electron microscopy, dynamic light scattering and laser Doppler velocimetry was performed. The genotoxicity studies were conducted using micronucleus and comet assays. Results showed that Y_2O_3 NP-induced significant DNA damage at higher dose (1000 mg kg^{-1} body weight) in peripheral blood leukocytes and liver cells, micronucleus formation in bone marrow and peripheral blood cells. The findings from biochemical assays depicted significant alterations in aspartate transaminase, alanine transaminase, alkaline phosphatase, malondialdehyde, superoxide dismutase, reduced glutathione, catalase and lactate dehydrogenase levels in serum, liver and kidneys at the higher dose only. Furthermore, tissue biodistribution of both particles was analyzed by inductively coupled plasma optical emission spectrometry. Bioaccumulation of yttrium (Y) in all tissues was significant and dose-, time- and organ-dependent. Moreover, Y_2O_3 NP-treated rats exhibited higher tissue distribution along with greater clearance through urine whereas Y_2O_3 MP-dosed animals depicted the maximum amount of Y in the feces. Hence, the results indicated that bioaccumulation of Y_2O_3 NPs via its Y ions may induce genotoxic effects.

KEYWORDS

biochemical, Biodistribution, genotoxicity, Wistar rats, yttrium oxide

1 | INTRODUCTION

Nanotechnology is a field of science that deals with nanoparticles (NPs) that have at least one dimension in 1–100 nm range. During the past 20 years, in nanoscience, scientists have achieved noteworthy success. NPs have different physical, chemical, electrical and optical properties than those of the microparticles (MPs). NPs are used in medical and commercial sectors including wastewater treatment, cosmetics and food industry (Kuppusamy, Yusoff, Maniam, & Govindan, 2016). Hence, nanotechnology has become a major factor in the world's economy and part of our everyday lives. However, there is also increasing concern that deliberate or inadvertent human and environmental exposure to NPs may lead to significant adverse effects (Oberdörster, Stone, & Donaldson, 2007). While nanotechnology and the production of NPs are growing exponentially, research into the toxicological impact and possible hazard of NPs to human health and the environment is still in its infancy. The questions concerning the side effects of products of nanotechnologies are relevant, since the potential of exposure to NPs increases as the quantity and types of NPs used in the society grow. To overcome all these debates and concerns, a new branch, nanotoxicology, has emerged years after the advent of nanotechnology, when various NPs had already been introduced into a number of industrial processes and products (Drobne, 2007). Several studies showed that NPs could induce the oxidative stress and production of reactive oxygen species (ROS) (Arooj et al., 2015; Jain, Reddy, Morales, Leslie-Pelecky, & Labhasetwar, 2008; Negahdary, Chelongar, Zadeh, & Ajdary, 2015; Park & Park, 2009; Prabhakar et al., 2012).

Among the known metal oxides yttrium oxide (Y_2O_3) NPs are notable because of their high free radical scavenging activity. The main technological applications of Y_2O_3 NPs are related with the optical industry (Bour, Reinholdt, Stepanov, Keutgen, & Kreibig, 2001).

Manufactured Y_2O_3 NPs are widely applied in materials, additives, synthesis, electrons and infrared-shielding (Andelman, Gordonov, Busto, Moghe, & Riman, 2010). Y_2O_3 NPs are used in imparting the red color in the picture tubes for televisions. In the field of material science, these particles are used in making plasma and flat panel displays. The red light emission property of Y_2O_3 NPs is used in making fluorescent lamps. Y_2O_3 NPs are utilized to make phosphors, iron garnets and high-temperature superconductors. They are also used as additives in the coatings used in high-temperature applications and in paints, plastics for guarding against ultraviolet degradation and in making permanent magnets. Some of the other applications of Y_2O_3 NPs are as additives in steel, non-ferrous alloys and iron. Y_2O_3 NPs can also be used as effective growth inhibitors in various microorganisms, making them applicable in diverse medical applications and antimicrobial control systems (Kannan & Sundrarajan, 2015). They also have certain neuroprotective properties that could be made use in biomedicine (Schubert, Dargusch, Raitano, & Chan, 2006). In 2014, global reserves of Y_2O_3 were estimated to be more than 500 000 tons according to Mineral commodity summaries 2015 (US Geological Survey, 2015). Y_2O_3 NPs are released into the environment from diesel engine emissions, improper disposal of automotive catalytic converters and improper disposal of old TV and computer monitors. These NPs may then make their way into air, soil or ground water (Biswas & Wu, 2005; Chow et al., 2005). Like many of the engineered NPs, Y_2O_3 NPs may also have toxic effects on humans and animals (Montanari & Gatti, 2016). However, the environmental effects of these NPs are still not completely known. The rapid rise of manufactured Y_2O_3 NPs raises concern of intentional and unintended delivery into the environment with possible implications for human and environmental health.

Previous toxicity studies with Y_2O_3 NPs are limited. A study revealed that when Y_2O_3 NPs were exposed to human aortic endothelial cells, a pronounced inflammatory response above a threshold concentration of 10 μg ml^{-1} was observed (Gojova et al., 2007). Effects of exposure to different types of Y_2O_3 NPs to human foreskin fibroblast cells demonstrated a concentration-dependent cytotoxicity was observed (Andelman et al., 2010). Y_2O_3 NP-induced dose- and time-dependent cytotoxicity that correlated with diminished cell survivability, cellular necrosis and an increase in cellular apoptosis when exposed to HEK293 cells (Selvaraj et al., 2014). Y_2O_3 nanoflowers exposed to rat primary hepatocyte cells caused decrease in cell viability, loss of lysosomal activity and membrane damage (Sönmez et al., 2015). Treatment with Y_2O_3 NPs showed that cell growth was significantly decreased and ROS levels were increased in marine phytoplanktons (Castro-Bugallo, González-Fernández, Guisande, & Barreiro, 2014). Y_2O_3 NPs produced cytotoxicity in a size- and dose-dependent manner in osteoblasts due to ROS generation (Zhou et al., 2016).

Current knowledge about the acute oral toxicity of Y_2O_3 NPs and MPs in rats is unknown. *In vivo* study of NPs is an important because animal systems are extremely complicated and the interaction of the NPs with biological systems could lead to novel biodistribution and clearance patterns (Fischer & Chan, 2007). Moreover, in mammals gastrointestinal tract is a crucial portal of entry of NPs. Hence, we have conducted acute oral dose toxicity study in albino Wistar female rats as per OECD guideline 420 (OECD, 2001) to get an idea about the doses used for the main genotoxicity studies. The characterization of NPs is necessary to interpret the potential toxicity of NPs to the biological system (Murdock, Braydich-Stolle, Schrand, Schlager, & Hussain, 2008). Hence, in the current investigation, the physicochemical properties of Y_2O_3 NPs and MPs were measured before conducting the animal experiments. To understand the mutations, cancer induction and the genotoxicity studies are important for the safety assessment of NPs. Genotoxicity assays such as the comet assay were carried out with peripheral blood leukocytes (PBL) and liver cells (Kumari, Kumari, Kamal, & Grover, 2014). Micronucleus test (MNT) was performed in peripheral blood (PB) cells (Çelik, Öğenler, & Çömelekoğlu, 2005) and bone marrow cells as per OECD guideline 474 (OECD, 2014). To estimate the alterations in biochemical indices such as Alanine aminotransferase (ALT), aspartate aminotransferase (AST), alkaline phosphatase (ALP), superoxide dismutase (SOD), catalase (CAT), glutathione content (GSH), lipid peroxidation (LPO) and lactate dehydrogenase (LDH) levels were evaluated in serum, liver and kidney tissues of treated rats. To detect pathological changes in tissues owing to NP treatment, histopathological investigations in liver, kidney, spleen, heart and brain were carried out. Metal content analysis of NPs is required to estimate the amount of NPs that enter into the target tissue or site. Hence, the effect of metal content in rat's whole blood, liver, kidney, heart, brain, spleen, lungs, urine and feces was also analyzed using inductively coupled plasma optical emission spectrometry (ICP-OES) to estimate the uptake and retention of NPs that enter target tissues or sites and for determining the anatomic fate, clearance and biological effect of these substances.

2 | MATERIALS AND METHODS

2.1 | Nanoparticles and chemicals

Y_2O_3 NPs (20–40 nm, 99.5%, product code: YN125), Y_2O_3 MPs (5–10 μm, 99.90%, product code: Y 1237) were purchased from Otto Chemie Pvt. Ltd. (Popatwadi, Mumbai, Maharashtra). Phosphate-buffered saline (Ca^{2+}, Mg^{2+}free; PBS), cyclophosphamide (CP), low melting agarose (LMA), normal melting agarose, NADH, sodium pyruvate, potassium chloride buffer, sulfosalicylic acid, potassium phosphate buffer, DTNB, perchloric acid and nitric acid were also purchased from Sigma Chemical Co. Ltd. (St. Louis, MO, USA). Sodium citrate, Giemsa stain was purchased from Himedia (Mumbai, India). All other chemicals and plastic ware were obtained locally and were of analytical reagent grade.

2.2 | Characterization of Y_2O_3 nanoparticles and Y_2O_3 microparticles

The particles were characterized by utilizing transmission electron microscopy (TEM), dynamic light scattering (DLS) and laser Doppler velocimetry (LDV) to assess the size of the materials, the state of dispersion, size distribution and zeta potential of the nanomaterials (NMs) in the Milli-Q water. Characterization of Y_2O_3 NPs and MPs was performed to evaluate the size and morphology utilizing TEM (JEM-2100; JEOL, Tokyo, Japan). The pictures were acquired from TEM with an accelerating voltage of 120 kV. The TEM was fitted with a plunge freezer and cryo-transfer holder to fix specimens in the frozen state and

equipped with a Gatan 2Kx2K CCD camera for getting high-resolution images. At a concentration of 0.01 mg ml^{-1}, particles were suspended in Milli-Q water and one drop of suspension was placed on a carbon-coated copper TEM grid and evaporated at room temperature. The software for advanced microscopy techniques was utilized for the digital TEM camera. This software was calibrated for nanoscale size quantifications for the precise examination of NPs. For the size quantification, 100 particles were calculated from arbitrary fields of view and images exhibiting the general morphology of the particles. The size and surface charge of the Y_2O_3 NPs in Milli-Q water suspension was quantified through DLS and LDV utilizing a Malvern Zetasizer Nano-ZS (Malvern Instruments, Malvern, UK). This device utilizes a 4 mW He–Ne 633 nm laser to analyze the samples and an electric field generator for the LDV quantifications. In Milli-Q water at the concentration of 40 μg ml^{-1}, the suspensions of freshly prepared Y_2O_3 NPs and MPs were ultrasonicated utilizing a probe sonicator (UPH100, Hielscher ultrasonics GmbH, Teltow, Germany) for 10 minutes at 90% amplitude. Further, the suspensions were diluted and adjusted to a lower concentration to acquire enough counts per second. The prepared samples were transferred to a 1.5 ml square cuvette for DLS quantifications and 1 ml of the suspension was transferred to a Malvern Clear Zeta Potential cell for the LDV quantification. The mean NP diameter was calculated using the same software program as utilized in the NP distribution and the polydispersity index (PdI) was used to quantify the size present in the solution. The PdI scale ranges from 0 to 1, where 0 corresponds to monodispersed and 1 corresponds to the polydispersed state of particles.

2.3 | Animals

Female albino Wistar rats, aged 6–8 weeks and weighing 80–120 g were obtained from the National Institute of Nutrition (Hyderabad, India). For 1 week, the animals were acclimatized in groups of five in polypropylene cages. A standard laboratory pellet diet (Unique autoclavable vegetal diet) was purchased from Scientific Animal Food and Engineering (SAFE, Augy, France), and fed to the animals then reverse osmosis water was provided ad libitum and maintained under standard conditions of humidity (55–65%), temperature (22 ± 3°C) and light (12-hour light/12-hour dark cycles). The Institutional Animal Ethics Committee (IAEC) approved the study (Ethical clearance number IICT/BIO/TOX/PG/28/11/14/09).

2.4 | Acute oral toxicity study

In accordance with the Organization for Economic Co-operation and Development (OECD) guidelines, the acute oral toxicity of Y_2O_3 NPs and MPs was assessed as per the "acute oral toxicity-fixed dose method" (OECD, 2001). A single rat was treated with an initial 5 mg kg^{-1} body weight (bw) dose according to the sighting study. In case of no adverse symptoms and mortality, a second rat received a 50 mg kg^{-1} bw dose, followed by 300 mg kg^{-1} bw dose and a final dose of 2000 mg kg^{-1} bw in sequence. Before dosing, rats were fasted overnight. In the sighting study, there were no apparent toxic symptoms and mortality at any dose level; therefore, a limit test was carried out with four female rats using 2000 mg kg^{-1} bw oral dose for Y_2O_3 NPs and Y_2O_3 MPs. After dosing, the test animals were kept under observation for a period of 14 days. During the observation period, the feed intake and bw were monitored daily. Mortality, signs and symptoms if any, were recorded twice on the day of dosing and once each day thereafter. The surviving animals were weighed at the end of the test period and they were killed by cervical dislocation at respective sampling times. Raw data of feed intake and bw were noted daily for 14 days and relative organ profile of tissues was recorded after treatment period. To assess the changes in the histopathology, tissues (heart, liver, kidneys, spleen and brain) were washed with 1% ice-cold saline and fixed in 10% neutral buffered formalin after being killed. In a Leica TP 1020 tissue processor (Leica Bio systems, Wetzlar, Germany), the formalin-fixed tissues were prepared and then implanted in paraffin blocks using Leica EG 1160 paraffin embedder. By using a Microm HM 360 microtome (Hyland Scientific, Stanwood, Washington, USA) the paraffin blocks were sliced into ribbons of 3 μm thickness and mounted on a glass microscope slide. After that, using a Microm HMS-70 stainer, slides were stained with hematoxylin and eosin and examined with Nikon Eclipse E 800 microscope (Nikon Instruments, Inc. Melville, New York, USA) at ×400 magnification. A minimum of three arbitrary sections per slide and at least three different fields were assessed for histopathological damage. To avoid bias, the slides were coded. One scorer analyzed the slides throughout the study.

2.5 | Experimental design: Genotoxicity, biochemical and biodistribution studies

Before every treatment of the rats, various doses of Y_2O_3 NPs and MPs were suspended in Milli-Q water. The doses were then ultrasonicated for 10 minutes at 90% amplitude, 100 W and 30 kHz using a probe sonicator (UPH 100; Hielscher ultrasonics GmbH, Teltow, Germany) for proper mixing before performing the investigation. The rats were arbitrarily divided into three groups (five rats in each group), positive control (for the genotoxicity studies), negative control and experimental groups. The three different doses of Y_2O_3 NPs and MPs were 250, 500 and 1000 mg kg^{-1} bw. The higher dose of 1000 mg kg^{-1} bw was chosen to see the toxic effect but not death or severe suffering in rats. After that, a descending sequence of dose levels (500 and 250 mg kg^{-1} bw) was selected with a view to demonstrating any dosage-related response and any no-observed-adverse effect level at the lowest dose level as per OECD guideline 420 (OECD, 2001). The control groups were treated with 2 ml kg^{-1} bw of Milli-Q water and the experimental groups were treated with Y_2O_3 NPs and MPs (250, 500 and 1000 mg kg^{-1} bw) through oral gavage. At a dose of 40 mg kg^{-1} bw, CP was used as positive control, which is a known mutagen. The desired volume was diluted up to 1 ml in Milli-Q water and administered intraperitoneally to rats under the positive control group. For the genotoxicity and biodistribution studies, the sampling times were 4, 24, 48 and 72 hours based on assay guidelines. For biochemical parameters, tissues samples were harvested at 24 and 72 hours post-treatment. Genotoxicity assay slides were randomized and coded to blind the scorer. All slides were scored by one person, to avoid inter-scorer variability.

2.6 | Comet assay

After acute exposure to the Y_2O_3 NPs and MPs, the alkaline comet assay was used for the evaluation of DNA damage in the rats. PBL

and liver samples were collected after dosing for 4, 24, 48 and 72 hours, and the assay was performed (Kumari et al., 2014). Blood withdrawal was done from the retro-orbital plexus of rats in EDTA-coated tubes. The liver tissue was removed from the rats after killing at various time intervals, minced and suspended at ~100 mg ml^{-1} in chilled homogenizing buffer (pH 7.5) and homogenized gently at a speed of 500–800 rpm. Cell viability in PBL and liver cells was determined by the trypan blue exclusion assay. For the comet assay, 10 µl of whole blood (10 000–30 000 lymphocytes) and liver homogenate was used for each slide preparation. For each experimental condition, three slides were prepared. In brief, microscope slides were pre-coated with 120 µl of 0.75% normal melting agarose in PBS and allowed to dry overnight at 37°C after placing a coverslip for a uniform layer. After pipetting 120 µl of 0.5% LMA containing blood cells on the pre-coated slides the second layer was prepared and dried at 4°C for 10 minutes. A third layer of plain 0.5% LMA (120 µl) was applied and a coverslip was quickly placed to get a uniform layer and dried at 4°C. After removing the coverslip, the slides were immersed in chilled lysis buffer (2.5 M NaCl, 0.1 M Na_2EDTA, 0.2 M NaOH, 1% Triton X-100, 10% dimethyl sulfoxide, pH 10.0) for 10 hours at 4°C. Next the slides were pre-soaked in alkaline buffer (10 M NaOH, 200 mM Na_2EDTA, pH >13.0) for 20 minutes and then electrophoresis was performed at 25 V adjusted at 300 mA for 20 minutes. The slides were neutralized twice in 0.4 M Tris buffer, pH 7.5, for 5 minutes and once in absolute methanol for 5 minutes. After staining with ethidium bromide (20 µg ml^{-1}) coded slides were scored using a fluorescence microscope (Olympus, Shinjuku-ku, Tokyo, Japan) with a blue (488 nm) excitation filter and yellow (515 nm) emission (barrier) filter at ×400 magnification. To measure the amount of DNA damage a total of 150 randomly selected cells per rat (50 cells per slide) were used and expressed as a percentage of DNA in the comet tail. Quantification of DNA breakage was carried out by using CASP software version 1.2.2 (Comet Assay Software; CaspLab, University of Wroclaw, Wroclaw, Poland) to calculate the amount of DNA damage and expressed as a percentage of DNA in the comet tail.

2.7 | Micronucleus test

After acute oral exposure for 24 and 48 hours with Y_2O_3 NPs and MPs, the bone marrow cells were extracted from the thigh bone of rats for conducting the MNT following the OECD guideline 474 (OECD, 2014). After aspiration into hypotonic solution of 1% sodium citrate, the bone marrow was removed from both femurs and centrifuged at approximately 112 g for 5 minutes. In a drop of 1% sodium citrate the cell pellet was resuspended and a smear was prepared on a microscope slide and allowed to dry in humidified air overnight. The MNT in PB cells was performed according to the protocol (Çelik et al., 2005) with some modifications. Whole blood was collected from retro-orbital plexus of each rat at 24 and 48 hours after the treatment from each group. On clean microscope slides, smears were prepared and air dried. In methanol, the slides were fixed for 2 minutes and then for 3 minutes stained with 0.5% Giemsa stain (prepared in PBS). The stained slides were evaluated for the assessment of the MN occurrence. Three slides were made for each animal. At ×1000 magnification, the slides were microscopically analyzed. Randomly, from three slides, 2000 polychromatic erythrocytes (PCEs) per animal were selected and the micronucleated PCEs frequencies (MN-PCEs) were recorded. In the bone marrow and PB cells, to determine the ratio of PCEs to normochromatic erythrocytes approximately 1000 cells from each animal were examined and the ratio was expressed as a percentage: (PCEs × 100/PCEs + normochromatic erythrocytes).

2.8 | Biochemical parameters

After acute oral treatment with 250, 500 and 1000 mg kg^{-1} bw doses of Y_2O_3 NPs and MPs, the whole blood samples were obtained by puncturing the retro-orbital plexus of rats. For biochemical estimations, the samples were collected in the tubes without using anticoagulant, which was then kept for 1 hour at room temperature. The serum thus obtained was then centrifuged at 176 g for 10 minutes. The liver and kidney of both control and treated rats were dissected out and washed in ice-cold saline, then with buffer of pH 7.4 (0.15 M Tris–HCl), dried and weighed. Tissues were homogenized separately in ice-cold sucrose (0.25 M) to make 10% homogenate (*w*/*v*) using a Miccra D-1 high-speed tissue homogenizer (MICCRA GmbH, Zienkener, Mullheim, Germany). The pellet was discarded, and the supernatant was used as an enzyme source. Serum, liver and kidney homogenates were used to analyze the AST, ALT, ALP, reduced GSH content, CAT, SOD, LDH and LPO. All the biochemical indices were estimated using a spectrophotometer (Spectramax Plus; Molecular Devices, Sunnyvale, CA, USA).

2.9 | Reduced glutathione content

The GSH content was analyzed in serum, liver and kidney. The quantity of GSH present was expressed as GSH in µg ml^{-1} of serum, GSH µg g^{-1} wet weight of tissue according to the protocol (Jollow, Mitchell, Zampaglione, & Gillette, 1974).

2.10 | Catalase

CAT activity in serum, liver and kidney homogenates was determined according to the protocol (Aebi, 1984). The decrease in absorbance was recorded for 1 minute at 240 nm. The enzyme activity was expressed as mmol of H_2O_2 decomposed per minute per milligram protein using a molar extinction coefficient of 43.6 M^{-1} cm^{-1}. The activity was expressed as units per milligram protein.

2.11 | Lactate dehydrogenase activity

The activity of LDH was estimated in the serum, liver and kidneys according to the procedure (McQueen, 1972). In a quartz cuvette, 1000 µl of Sorensen phosphate buffer, 100 µl NADH and 20 µl of serum was added and mixed well. Next, 150 µl sodium pyruvate was added and again mixed well. The absorbance was measured at 340 nm at 10 seconds interval for 2 minutes using a spectrophotometer. The LDH activity was expressed as µmol h^{-1} ml^{-1} using molar extinction coefficient of 6.3 mM^{-1} cm^{-1}.

2.12 | Lipid peroxidation

Malondialdehyde (MDA), which is the end product of LPO, was measured in serum, kidney and liver tissue homogenate according to

the procedure (Wills, 1969). The reaction of serum and tissue homogenates with thiobarbituric acid and 15% of trichloroacetic acid reagent resulted in the formation of the thiobarbituric acid–MDA complex. The absorbance of this end product (pink colored) was estimated at 532 nm. The quantity of MDA was determined using a molar extinction coefficient of 1.56×10^5 M^{-1} cm^{-1} and expressed as nanomoles of MDA formed per gram wet weight of the tissue in liver, kidney and nanomoles of MDA per milliliter in serum. Protein was determined according to the protocol (Lowry, Rosebrough, Farr, & Randall, 1951).

2.13 | Superoxide dismutase

SOD activity was estimated in the serum, liver and kidneys using the method (Marklund & Marklund, 1974). A 3 ml aliquot of assay mixture contained 50 mM Tris–HCl buffer (pH 8.2) with 1 mM diethylene triamine penta acetic acid, 45 µl of 10 mM pyrogallol in 10 mM HCl and 10 µl of tissue supernatant. The rate of inhibition of pyrogallol auto-oxidation after the addition of enzyme extract was noted at 420 nm. The amount of enzyme required to give 50% inhibition of pyrogallol auto-oxidation was considered as one unit of enzyme activity. The enzyme activity was expressed as units per milligram protein. The protein content was estimated using standard protocol (Lowry et al., 1951). Bovine serum albumin was used as standard.

2.14 | Aspartate aminotransferase and alanine aminotransferase activity

The activity of AST and ALT enzyme levels were measured in serum as well as in liver and kidney according to the procedure (Yatzidis, 1960). AST and ALT activities were expressed as micromole per hour per milliliter in serum and micromole per hour per milligram protein in liver and kidney respectively.

2.15 | Alkaline phosphatase activity assay

The activity of ALP was determined following p-nitrophenyl phosphate method described in the diagnostic kit from Siemens Ltd. (Vadodara, Gujarat, India). This method utilizes p-nitrophenyl phosphate that is hydrolyzed by ALP into a yellow-colored product p-nitrophenol having maximum absorbance at 405 nm. The rate of reaction is directly proportional to the enzyme activity. The absorbance of the test was read against a blank at 405 nm at intervals of 30 seconds for 2 minutes using a spectrophotometer (Spectra Max Plus; Molecular Devices). The enzyme activity was expressed as activity of ALP (µmol p-nitrophenol min^{-1} ml^{-1}) using the molar extinction coefficient of 18.75 mM^{-1} cm^{-1}.

2.16 | Yttrium content analysis in tissues

A biodistribution study of the Y_2O_3 NPs and MPs in the female Wistar rats was carried out in rat whole blood, liver, kidneys, heart, brain, spleen, urine and feces. The animals were placed in metabolic cages after treatment to collect the urine and feces samples and these samples were collected after 4, 24, 48 and 72 hours of dosing. The samples were processed using the method in Gómez, Sánchez, Llobet, Corbella, and Domingo (1997). The samples were pre-digested in nitric acid overnight, and then heated at 80°C for 10 hours, followed by additional heating at 130–150°C for 30 minutes. Subsequently, a volume of 0.5 ml of 70% perchloric acid was added, the samples were then again heated again for 4 hours and evaporated nearly to dryness. Following digestion, the samples were filtered and 2% HNO_3 was added to a final volume of 5 ml for analysis. The standard solution of Y was serially diluted to 100, 50, 10, 1 ppm. The wavelength of 418.66 nm was found to get intensity of the samples. The Y content in the samples was determined using ICP-OES (JY Ultima, Jobin Vyon, France).

2.17 | Statistical analysis

The statistical significant changes between treated and control groups were analyzed by two-way ANOVA. All results were expressed as mean and standard deviation (mean ± SD) of the mean. Multiple pairwise comparisons were done using the Bonferroni post-test to compare replicate means by row and Student's *t*-test was used to verify the significance of positive response. Statistical analyses were performed using GraphPad Prism 5 Software package for windows (GraphPad Software, Inc., La Jolla, CA, USA). The statistical significance for all tests was set at $P < 0.01$.

3 | RESULTS

3.1 | Characterization of Y_2O_3 nanoparticles and Y_2O_3 microparticles

The physicochemical characteristics of Y_2O_3 particles were determined by TEM, DLS and LDV analysis. The data obtained are shown in Table 1 . Over 100 particles were measured in random fields to calculate the mean size of Y_2O_3 NPs and Y_2O_3 MPs using TEM. The size obtained for Y_2O_3 NPs and Y_2O_3 MPs was 83.63 ± 17.48 nm (Figure 1B) and 1.50 ± 41.295 µm (Figure 1A), respectively. The TEM micrographs also show the aggregated nature of particles with different shape and sizes. The hydrodynamic diameter and PdI of Y_2O_3 NPs in Milli-Q water suspension obtained by DLS was 159.2 ± 1.2 and 0.817 respectively. The larger hydrodynamic diameter than the TEM size indicated that Y_2O_3 NPs formed larger agglomerates in aqueous suspension than in the dry state. Zeta potential (ζ) and electrophoretic mobility of Y_2O_3 NPs was quantified by LDV and found to be 8.83 mV and 0.69 µm cm^{-1} s^{-1} V respectively at pH 7.0. In case of Y_2O_3 MPs, DLS and LDV data were found to be out of the detection limit.

3.2 | Animal observation, food consumption, body weight, organ weight and histopathological examination

During the 14-day observation period after single oral treatment of rats with 5, 50, 300 and 2000 mg kg^{-1} bw of Y_2O_3 NPs and MPs, adverse signs, symptoms or mortality were not noticed. However, rats treated with 2000 mg kg^{-1} bw of Y_2O_3 NPs showed dullness, irritation and moribund symptoms. Further, both NP- and MP-treated rats showed no significant changes in bw, feed intake and relative organ weight were shown in Tables 2–4. At the end of the acute oral toxicity study, various tissues such as liver, kidney, heart, spleen and brain were

TABLE 1 Characterization of Y_2O_3 NPs and MPs

Particles	Size using TEM	DLS		LDV		
		Average diameter (nm)	PdI	Zeta potential (mV)	Electrophoretic mobility (μm cm^{-1} s^{-1} V)	pH
Y_2O_3 NPs (nm)	83.63 ± 17.48	159.2 ± 1.2	0.817	8.83	0.69	7.0
Y_2O_3 MPs (μm)	1. 50 ± 41.295	ND	ND	ND	ND	7.0

DLS, dynamic light scattering; LDV, laser Doppler velocimetry; MPs, microparticles; ND, not detected; NPs, nanoparticles; PdI, polydispersity index.

Y_2O_3 NPs and MPs at the concentration of 40 μg ml^{-1} were dispersed in Milli-Q water and mixing was done via probe sonication for 10 minutes just before estimations.

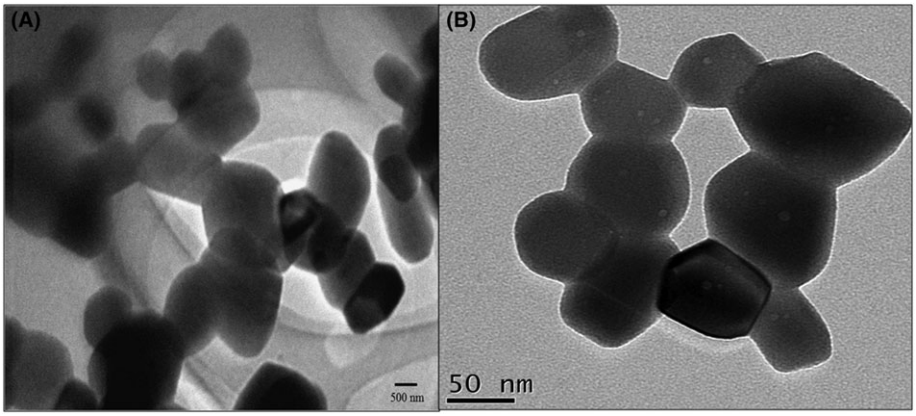

FIGURE 1 Transmission electron microscopy image of (a) Y_2O_3 microparticles and (B) Y_2O_3 nanoparticles in Milli-Q water mixing done via probe sonication for 10 minutes by transmission electron microscopy

TABLE 2 Effect of Y_2O_3 MPs and NPs on body weight profile

Treatments	Dose (mg kg^{-1} bw)	Zero day	3rd day	7th day	10th day	14th day
Control*	–	126 ± 9.71	134 ± 11.5	138 ± 10.7	142 ± 12	146 ± 13.6
Y_2O_3 MPs	250	124 ± 11.2	130 ± 12.4	136 ± 11.4	140 ± 13.2	144 ± 14.14
	500	122 ± 12.1	132 ± 13.1	134 ± 12.8	138 ± 13.4	142 ± 13.9
	1000	121.5 ± 10.5	134 ± 13.3	133.5 ± 13.3	137.5 ± 12.9	141.5 ± 13.2
Y_2O_3 NPs	250	122 ± 11.5	129 ± 12.6	137 ± 12.9	137.5 ± 12.6	143 ± 12.2
	500	124 ± 11	130 ± 12.7	134 ± 13	138 ± 13.4	141 ± 13.2
	1000	126 ± 11.5	132 ± 12.9	139 ± 12.2	140 ± 13	141 ± 13.2

MPs, microparticles; NPs, nanoparticles.

*Milli-Q water (negative control).

Data represented as mean ± SD, *n* = 5 animals per group.

TABLE 3 Effect of Y_2O_3 MPs and NPs on feed intake profile

Treatments	Dose (mg kg^{-1} bw)	1st day	3rd day	7th day	10th day	14th day
Control*	–	10.1 ± 0.71	11.2 ± 0.97	13.8 ± 1.10	14.8 ± 1.28	15.2 ± 1.32
Y_2O_3 MPs	250	11.4 ± 1.15	11.4 ± 1	13.6 ± 1.2	14.4 ± 1.26	15.4 ± 1.40
	500	11.4 ± 1.07	11.8 ± 1.13	13.2 ± 1.15	14.1 ± 1.32	15.6 ± 1.32
	1000	11.3 ± 1.10	12.1 ± 1.13	12.9 ± 1.16	14.2 ± 1.15	15.5 ± 1.27
Y_2O_3 NPs	250	11.4 ± 0.81	11.5 ± 0.89	12.9 ± 1.20	14.4 ± 1.16	15.2 ± 1.31
	500	11.5 ± 1	12.2 ± 1.14	12.6 ± 1.23	14.7 ± 1.28	15.6 ± 1.39
	1000	11.5 ± 0.92	12.3 ± 1	12.6 ± 1.07	14.6 ± 1.22	16.1 ± 1.40

MPs, microparticles; NPs, nanoparticles.

*Milli-Q water (negative control).

Data represented as mean ± SD, *n* = 5 animals per group.

studied for histopathological study using hematoxylin and eosin stain. All the tissue sections were evaluated for any toxic changes as well as presence of any extraneous material deposits. The histomicrographs of liver and kidney tissues showed a focal area of necrosis and tubular necrosis respectively, with exposure to Y_2O_3 NPs in 2000 mg kg^{-1} bw (high) dose groups (Figure 2B,D). However, there were no abnormal

TABLE 4 Effect of Y_2O_3 MPs and NPs on relative organ weight profile after 14 days of single oral treatment

Treatments	Dose (mg kg^{-1} bw)	Liver	Lung	Kidney	Brain	Spleen	Heart
Control*	–	5.11 ± 0.34	1.21 ± 0.24	0.75 ± 0.08	1.62 ± 0.09	0.66 ± 0.13	0.76 ± 0.05
Y_2O_3 MPs	250	5.12 ± 0.50	1.22 ± 0.32	0.75 ± 0.19	1.62 ± 0.21	0.66 ± 0.10	0.76 ± 0.12
	500	5.13 ± 0.61	1.22 ± 0.33	0.75 ± 0.32	1.62 ± 0.19	0.67 ± 0.34	0.76 ± 0.88
	1000	5.13 ± 0.64	1.23 ± 0.30	0.76 ± 0.55	1.62 ± 0.37	0.67 ± 0.71	0.77 ± 0.10
Y_2O_3 NPs	250	5.14 ± 0.52	1.23 ± 0.06	0.76 ± 0.58	1.62 ± 0.21	0.67 ± 0.07	0.76 ± 0.33
	500	5.15 ± 0.49	1.24 ± 0.23	0.76 ± 0.77	1.63 ± 0.18	0.67 ± 0.59	0.77 ± 0.46
	1000	5.17 ± 0.50	1.25 ± 0.23	0.77 ± 0.96	1.63 ± 0.49	0.68 ± 0.09	0.77 ± 0.72

MPs, microparticles; NPs, nanoparticles.

*Milli-Q water (negative control).

Data represented as mean ± SD, n = 5 animals per group.

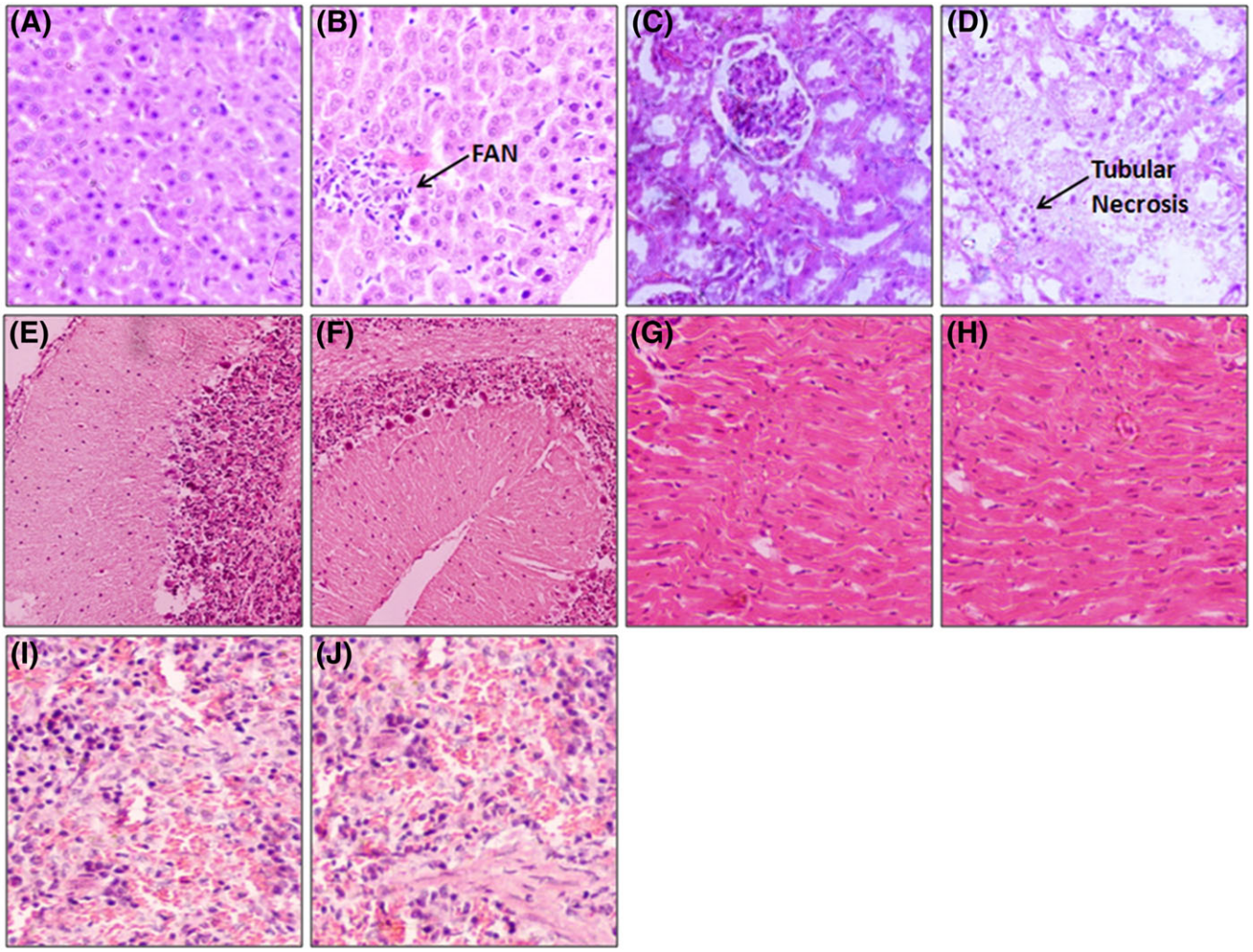

FIGURE 2 Histopathology of liver, kidneys, brain, heart and spleen tissues of rats after single oral treatment with 2000 mg kg^{-1} bw Y_2O_3 nanoparticles. A, C, E, G and I respectively showing the normal architecture of liver, kidney, brain, heart, and spleen of control rats. (B) FAN in liver (D). Tubular necrosis in the kidney (F), (H) and (J) revealing no pathological alterations in brain, heart, and spleen of Y_2O_3 NP-treated group at ×400 magnification. FAN, focal area of necrosis.

pathological changes in brain, heart and spleen tissues with 2000 mg kg^{-1} bw (Figure 2F,H,J). The sections of control liver, kidneys, heart, brain and spleen have been shown in Figure 2A, C, E, G and I, respectively. However, the tissues of rats exposed to 5, 50 and 300 mg kg^{-1} bw of Y_2O_3 NPs and all the doses of Y_2O_3 MPs revealed normal architecture of liver, kidneys, spleen, brain and heart tissues (data not shown). Hence, the acute toxicity of these compounds was greater than 2000 mg kg^{-1} bw, ranking these substances into category 5, as per OECD (2001) guidelines and the globally harmonized system. The criteria for hazard category 5 are intended to enable the identification of test substances, which are of relatively low acute toxicity hazard but which, under certain circumstances, may present a danger to vulnerable populations. These substances are anticipated to have an oral LD_{50} in the range of 2000–5000 mg kg^{-1} bw.

3.3 | Genotoxicity studies

3.3.1 | Comet assay

The results obtained from the comet assay after acute oral treatment with 250, 500 and 1000 mg kg^{-1} bw doses of Y_2O_3 NPs and MPs in rats are depicted in Figure 3(A,B). In all samples of PBL and liver cells, the cell viability by the trypan blue exclusion assay ranged from 90% to 94% (data not shown). When the CP (positive control) was compared with the negative control, a significant difference in percentage of tail DNA was noted confirming the test efficacy for detecting DNA damaging agents. A clear induction of DNA damage was observed at 24 hours post-treatment by CP. A statistically significant increase in percentage tail DNA was observed in PBL and liver cells of rats treated with the highest dose of 1000 mg kg^{-1} bw of Y_2O_3 NPs at 24 and 48 hour sampling times. However, at the 4 and 72 hour sampling times no significant DNA damage was observed at any dose. Moreover, in PBL and liver cells treated with Y_2O_3 MPs did not induce significant DNA damage at all doses and time intervals.

3.3.2 | Micronucleus test

The bone marrow MNT was conducted after 24 and 48 hours of oral treatment with 250, 500 and 1000 mg kg^{-1} bw of Y_2O_3 NPs and MPs in female Wistar rats. After 24 and 48 hours the MNT data indicated a statistically significant increment in the MN-PCE frequency in the Y_2O_3 NP-treated groups with only the higher dose of 1000 mg kg^{-1} bw in rats. However, Y_2O_3 MP-treated groups did not show any significant increase in the frequency of MN-PCEs. On the other hand, on MN-PCE frequency the CP-treated group induced a substantially significant effect. In comparison to the negative control rats, the various doses of Y_2O_3 NPs and MPs exhibited an insignificant decrease in percentage PCEs with the MNT (Table 5). Similarly, the MNT was carried out in PB cells after 24 and 48 hours of acute oral treatment with all the three doses of Y_2O_3 NPs and MPs. Significant changes in MN-PCEs in the Y_2O_3 NP-treated group was observed only after 24 and 48 hours at 1000 mg kg^{-1} bw. The positive control rats treated with CP induced significant changes in MN-PCEs and percentage PCEs as well. All doses of Y_2O_3 NPs and MPs exhibited insignificant decrease in percentage PCEs in comparison to the negative control rats (Table 6).

3.4 | Biochemical parameters

After 24 and 72 hours of oral treatment with 250, 500 and 1000 mg kg^{-1} bw of Y_2O_3 NPs and MPs in rats, the levels of MDA were significantly enhanced at 1000 mg kg^{-1} bw of Y_2O_3 NPs in the serum,

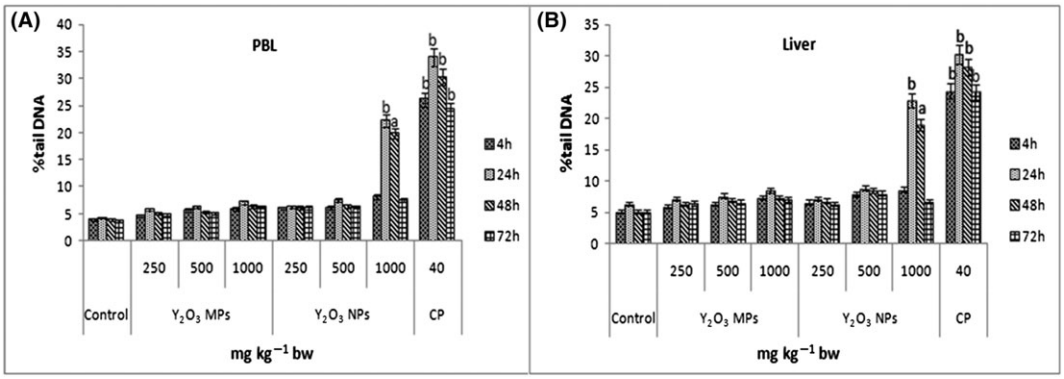

FIGURE 3 In vivo comet assay of Y_2O_3 NPs and Y_2O_3 MPs. Mean % tail DNA in (A) PBLs and (B) liver cells of female Wistar rats after single oral treatment with Y_2O_3 NPs and Y_2O_3 MPs at 4, 24, 48, 72 hours. Deionized water (control); CP as a positive control. Data represented as mean ± SD significantly different from control at $^aP < 0.01$ and $^bP < 0.001$, $n = 5$ animals per group. CP, cyclophosphamide; MPs, microparticles; NPs, nanoparticles; PBLs, peripheral blood leukocytes.

TABLE 5 Frequency of MN-PCEs and percentage PCEs in female bone marrow cells treated with Y_2O_3 NPs and MPs at 24 and 48 h

		24 h		48 h	
Treatments	Dose (mg kg^{-1} bw)	MN-PCEs	% PCEs	MN-PCEs	% PCEs
Control*	–	4.45 ± 0.55	41.65 ± 1.55	4.55 ± 0.65	34.4 ± 2
Y_2O_3 NPs	250	3.22 ± 0.62	40.9 ± 1.3	4.4 ± 0.2	36.7 ± 2.8
	500	4.2 ± 0.6	40.2 ± 2.9	4.25 ± 0.35	38.15 ± 2.55
	1000	10.2 ± 0.9**	36.8 ± 2.0	10.03 ± 0.7**	36.65 ± 2.85
Y_2O_3 MPs	250	2.82 ± 0.58	42.95 ± 1.75	3.35 ± 0.65	34.55 ± 3.05
	500	3.32 ± 0.5	44.7 ± 2.5	4.05 ± 0.75	33.85 ± 2.65
	1000	4.01 ± 0.5	42.85 ± 2.35	5.3 ± 0.7	30.65 ± 3.05
CP†	40	31.8 ± 0.6***	22.2 ± 1.7***	29.25 ± 0.95***	20.7 ± 2.1***

CP, cyclophosphamide; MN, micronucleus; MPs, microparticles; NPs, nanoparticles; PCEs, polychromatic erythrocytes.

*Milli-Q water (negative control).

†Positive control.

Data represented as mean ± SD, significantly different from control. **$P < 0.01$ and ***$P < 0.001$, $n = 5$ animals per group.

TABLE 6 The frequency of MN-PCEs and percentage PCEs in female rat peripheral blood cells treated with Y_2O_3 NPs and MPs at 24 and 48 h

Treatments	Dose (mg kg^{-1} bw)	24 h		48 h	
		MN-PCEs	% PCEs	MN-PCEs	% PCEs
Control*	–	2.1 ± 0.2	3.6 ± 0.7	2.11 ± 0.46	3.5 ± 0.7
Y_2O_3 NPs	250	2.12 ± 0.48	3.5 ± 0.6	2.09 ± 0.5	3.4 ± 0.7
	500	2.13 ± 0.47	3.4 ± 1.2	2.11 ± 0.51	3.3 ± 0.7
	1000	2.31 ± 0.59**	3.52 ± 0.62	2.29 ± 0.53**	3.31 ± 0.81
Y_2O_3 MPs	250	2.11 ± 0.49	3.45 ± 0.75	2.09 ± 0.45	3.45 ± 0.75
	500	2.14 ± 0.46	3.35 ± 0.45	2.15 ± 0.46	3.45 ± 0.75
	1000	2.16 ± 0.44	3.6 ± 0.7	2.12 ± 0.4	3.49 ± 1.09
CP†	40	11.0 ± 0.5***	1.6 ± 0.3***	10.9 ± 0.3***	1.7 ± 0.9***

CP, cyclophosphamide; MN, micronucleus; MPs, microparticles; NPs, nanoparticles; PCEs, polychromatic erythrocytes.

*Milli-Q water (negative control).

†Positive control.

Data represented as mean ± SD, significantly different from control. **P < 0.01 and ***P < 0.001, n = 5 animals per group.

liver and kidneys (Figure 4). CAT levels were increased (Figure 5) and GSH, SOD levels were significantly decreased (Figures 6 and 7) when treated with the dose of 1000 mg kg^{-1} bw Y_2O_3 NPs at 24 and 72 hours compared to control rats in the serum, liver and kidneys. LDH activity was recorded to be statistically significant than the control values at 1000 mg kg^{-1} bw of NPs in the serum, liver and kidneys (Figure 8). However, levels of MDA, GSH, SOD, CAT and LDH at all doses of Y_2O_3 MPs and 250 and 500 mg kg^{-1} bw of NPs were statistically non-significant compared to control group of rats. Significant increases in AST and ALT levels in serum, liver and decreases in AST and ALT levels in kidney at the 24- and 72 hour sampling times at 1000 mg kg^{-1} bw dose of Y_2O_3 NPs (Figures 9 and 10). The activity of ALP in serum increased significantly at 1000 mg kg^{-1} bw dose of Y_2O_3 NPs after both exposure periods, i.e. 24 and 72 hours (Figure 11). Alterations in serum, liver and kidney AST, ALT and ALP at all doses of Y_2O_3 MPs and 250 and 500 mg kg^{-1} bw of NPs were statistically non-significant compared to control group of rats.

3.5 | Biodistribution of Y_2O_3 nanoparticles and microparticles

The biodistribution levels of Y after acute oral exposure of Y_2O_3 NPs and MPs at 4, 24, 48 and 72 hours with various doses of 250, 500 and 1000 mg kg^{-1} bw in female Wistar rats were analyzed by ICP-

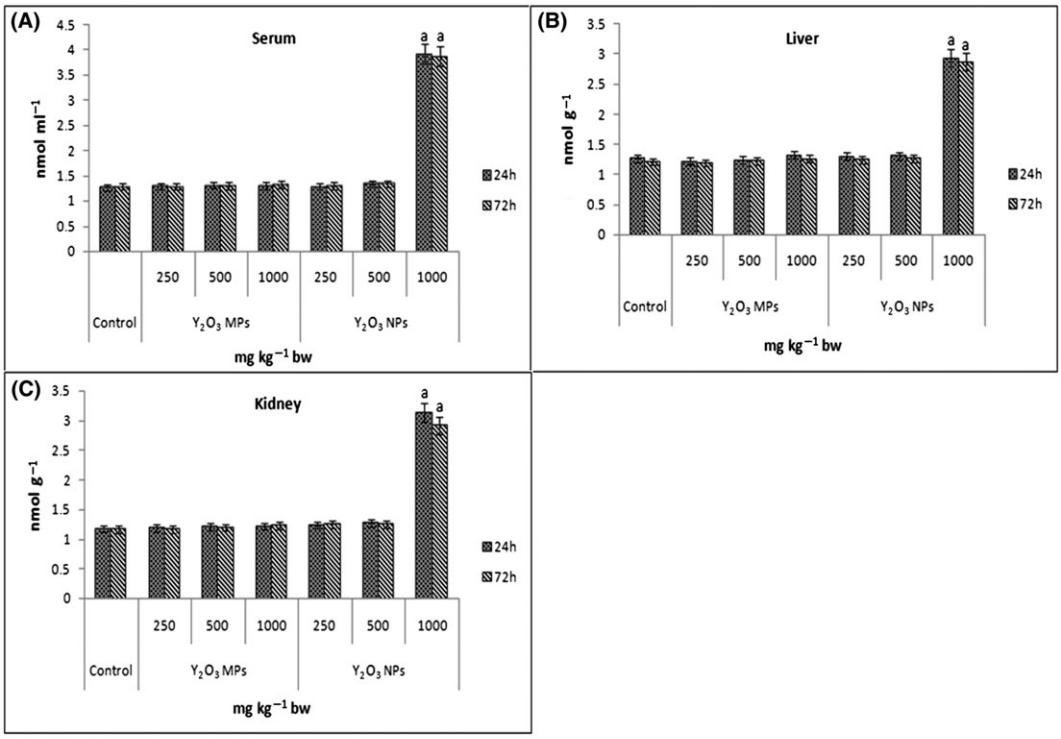

FIGURE 4 Alterations in malondialdehyde levels in (A) serum, (B) liver and (C) kidney after 24 and 72 hours of single oral treatment with Y_2O_3 NPs and Y_2O_3 MPs. Data represented as mean ± SD, significantly different from control at $^a P$ < 0.001, n = 5 animals per group. MPs, microparticles; NPs, nanoparticles.

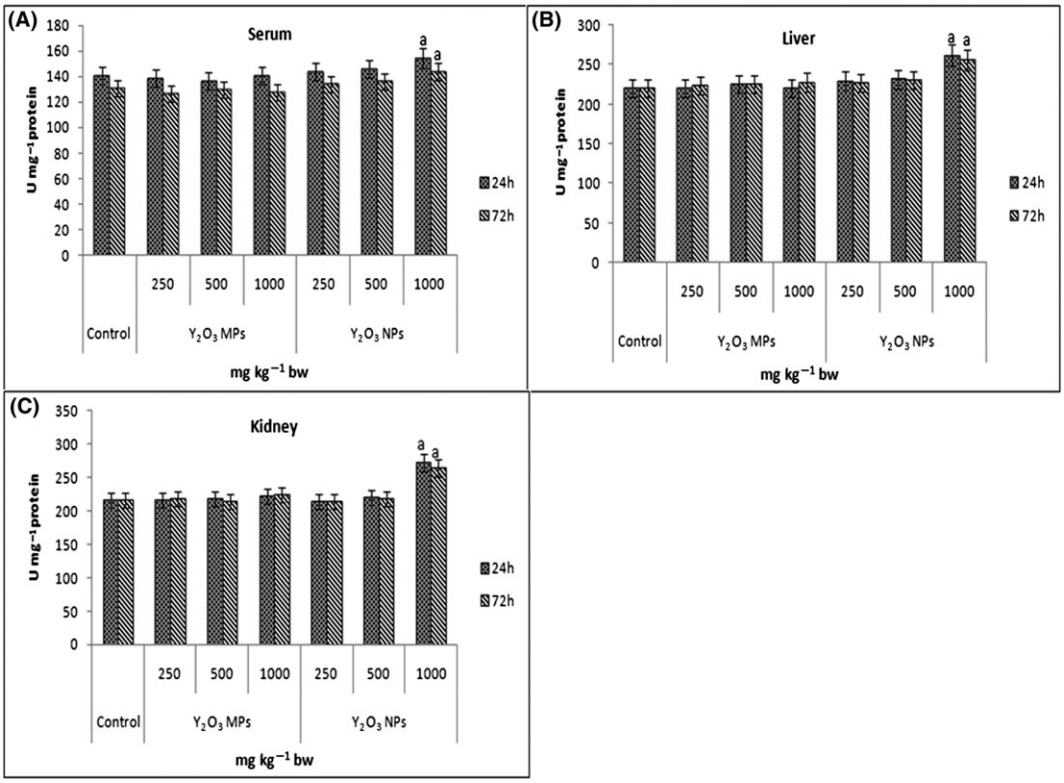

FIGURE 5 Alterations in catalase levels in (A) serum, (B) liver and (C) kidney after 24 and 72 hours of single oral treatment with Y_2O_3 NPs and Y_2O_3 MPs. Data represented as mean ± SD, significantly different from control at $^aP < 0.001$, $n = 5$ animals per group. MPs, microparticles; NPs, nanoparticles.

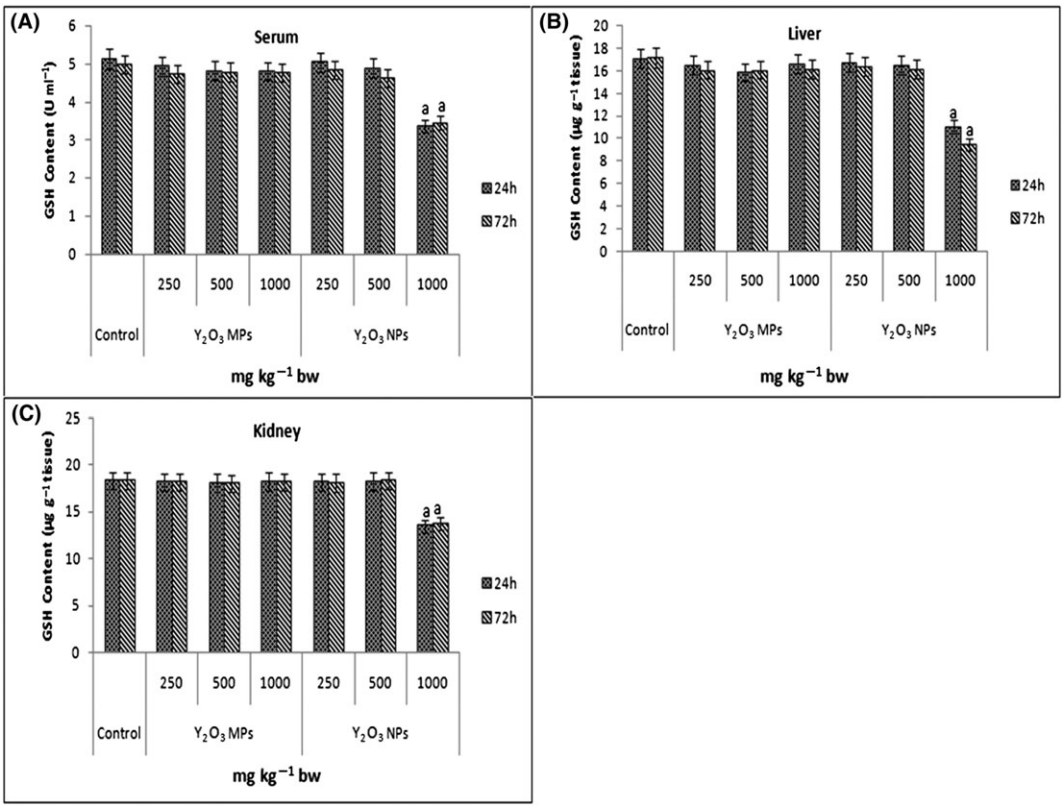

FIGURE 6 Alterations in GSH levels in (A) serum, (B) liver and (C) kidney after 24 and 72 hours of single oral treatment with Y_2O_3 NPs and Y_2O_3 MPs. Data represented as mean ± SD, significantly different from control at $^aP < 0.001$, $n = 5$ animals per group. GSH, glutathione; MPs, microparticles; NPs, nanoparticles.

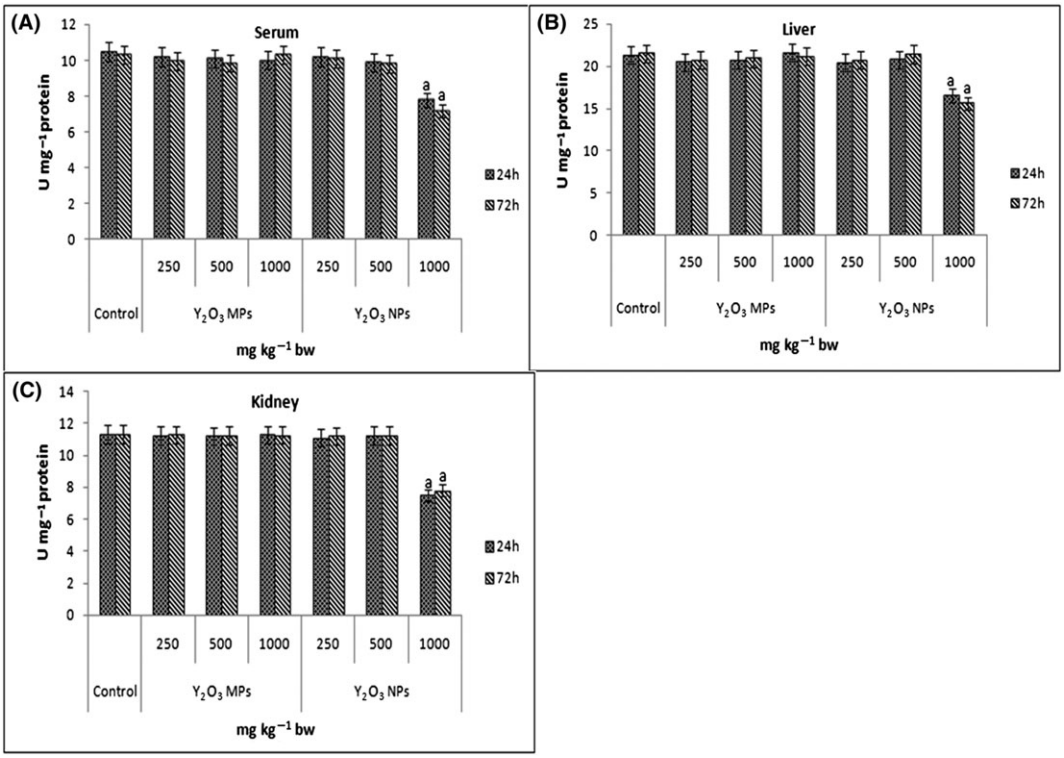

FIGURE 7 Alterations in superoxide dismutase levels in (A) serum, (B) liver and (C) kidney after 24 and 72 hours of single oral treatment with Y_2O_3 NPs and Y_2O_3 MPs. Data represented as mean ± SD, significantly different from control at $^aP < 0.001$, $n = 5$ animals per group. MPs, microparticles; NPs, nanoparticles.

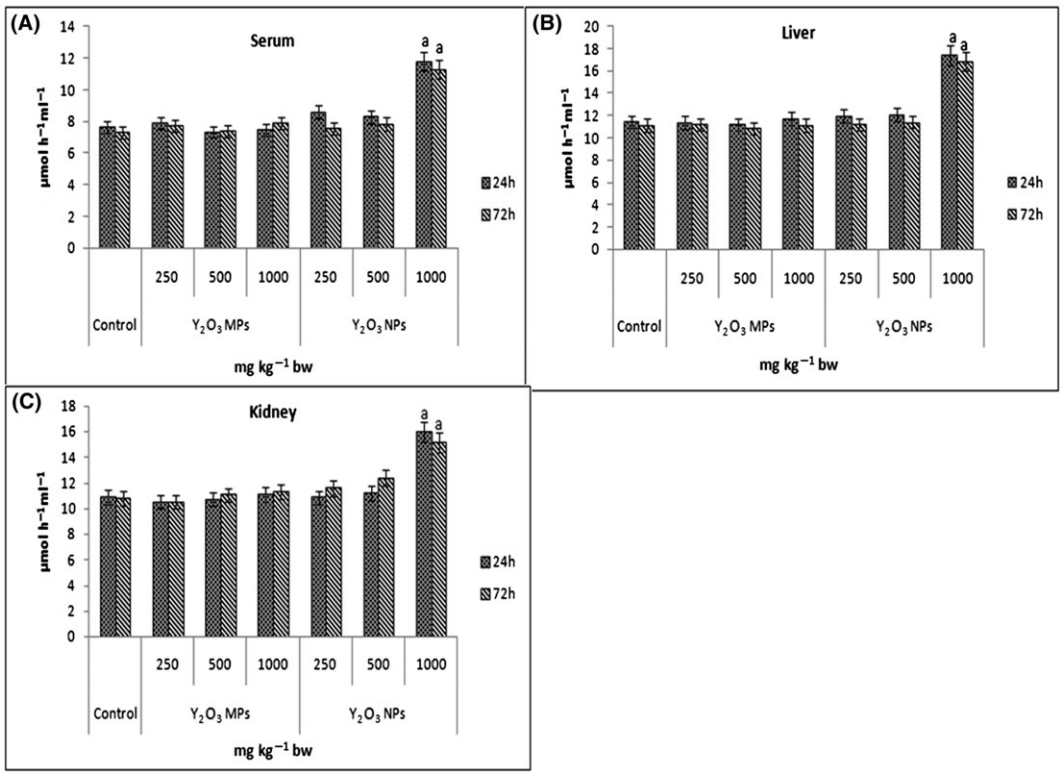

FIGURE 8 Alterations in lactic dehydrogenase levels in (A) serum, (B) liver and (C) kidney after 24 and 72 hours of single oral treatment with Y_2O_3 NPs and Y_2O_3 MPs. Data represented as mean ± SD, significantly different from control at $^aP < 0.001$, $n = 5$ animals per group. MPs, microparticles; NPs, nanoparticles.

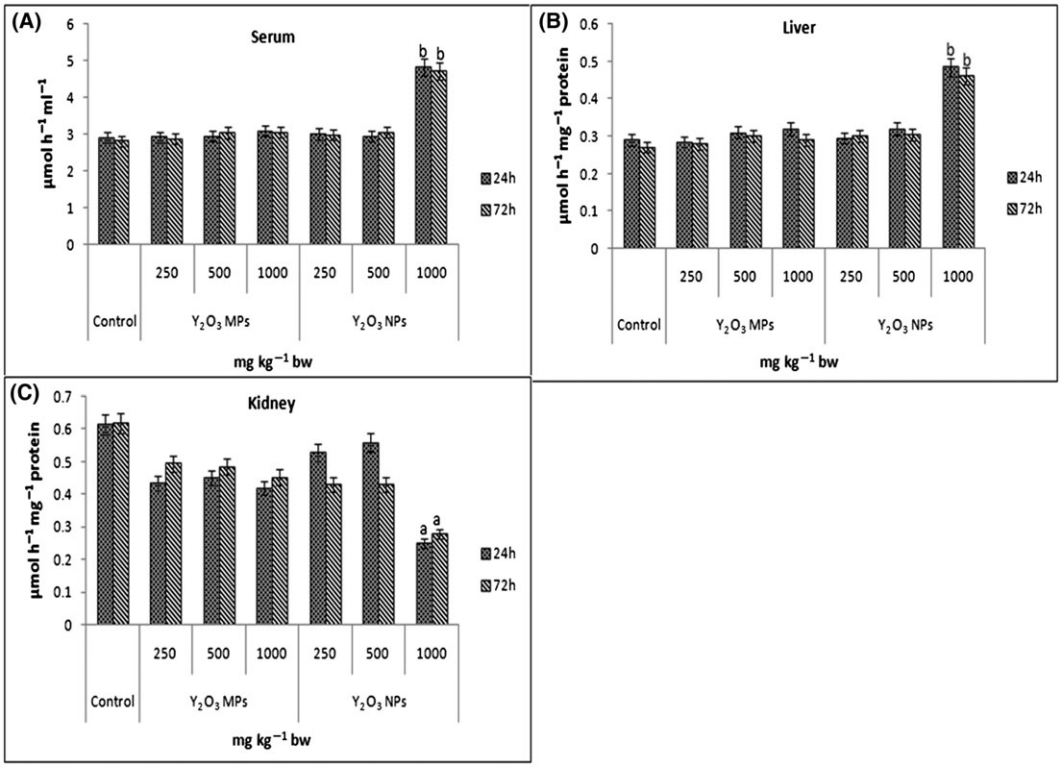

FIGURE 9 Alterations in aspartate aminotransferase levels in (A) serum, (B) liver and (C) kidney after 24 and 72 hours of single oral treatment with Y_2O_3 NPs and Y_2O_3 MPs. Data represented as mean ± SD, significantly different from control at $^aP < 0.01$ and $^bP < 0.001$, $n = 5$ animals per group. MPs, microparticles; NPs, nanoparticles.

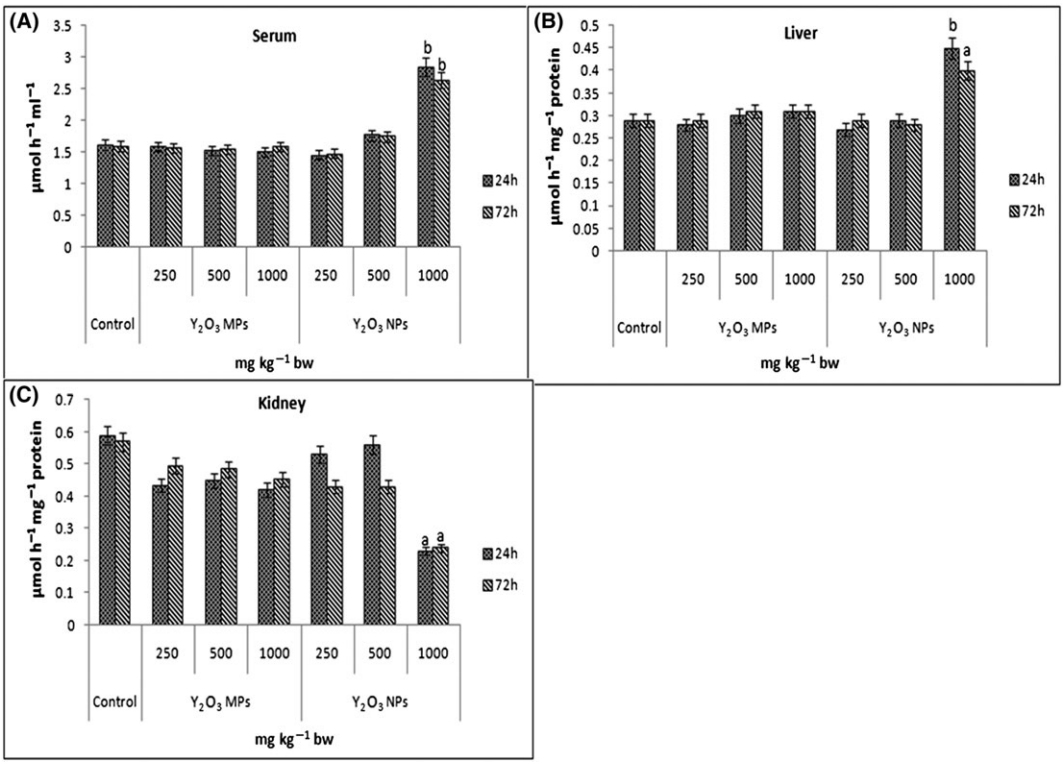

FIGURE 10 Alterations in alanine aminotransferase levels in (A) serum, (B) liver and (C) kidney after 24 and 72 hours of single oral treatment with Y_2O_3 NPs and Y_2O_3 MPs. Data represented as mean ± SD, significantly different from control at $^aP < 0.01$ and $^bP < 0.001$, $n = 5$ animals per group. MPs, microparticles; NPs, nanoparticles.

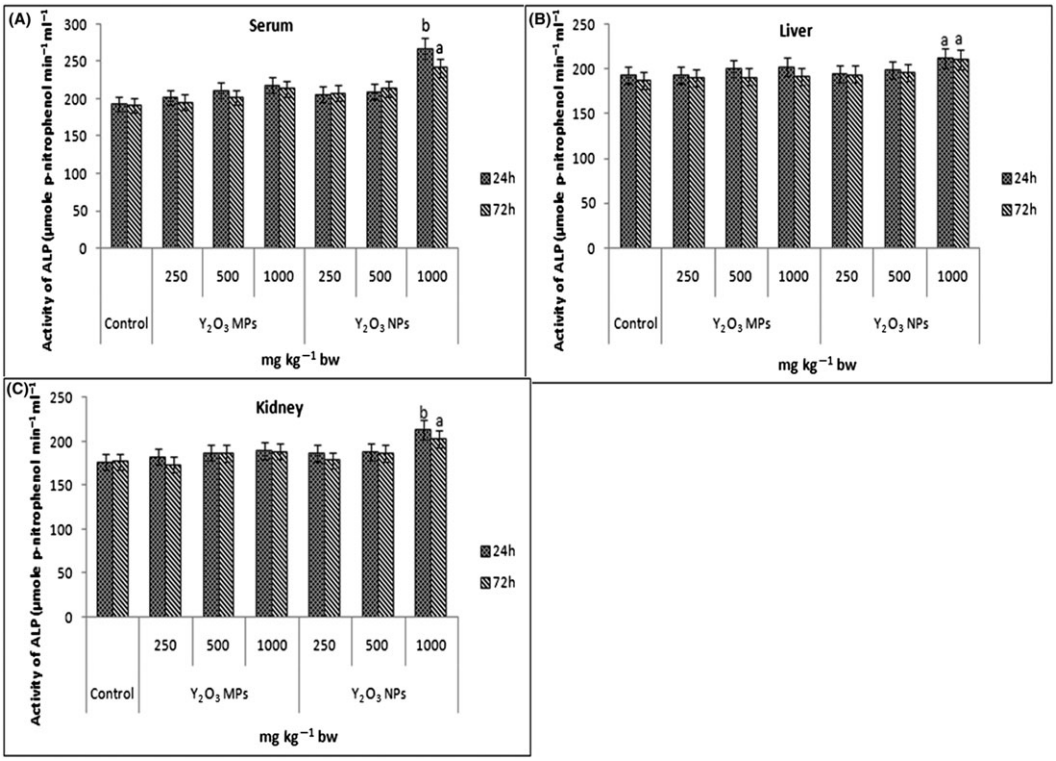

FIGURE 11 Alterations in ALP levels in (A) serum, (B) liver and (C) kidney after 24 and 72 hours of single oral treatment with Y_2O_3 NPs and Y_2O_3 MPs. Data represented as mean ± SD, significantly different from control at $^aP < 0.01$ and $^bP < 0.001$, $n = 5$ animals per group. ALP, alkaline phosphatase; MPs, microparticles; NPs, nanoparticles.

OES. The results revealed that a significant accumulation of Y in liver, kidneys, spleen, lung, heart, brain and whole blood in rats treated with 1000 mg kg^{-1} bw dose of NPs at all time periods (Figure 12A–I). At 500 mg kg^{-1} bw dose, the significant accumulation of Y was observed in the liver, kidney, spleen and lungs at all time points, whereas at 24 and 48 hours, the significant accumulation of Y in the heart was found. In the case of kidneys, there was a significant accumulation at the 250 mg kg^{-1} bw dose of NP-treated rats (Figure 12B) at the 4- and 24-hour sampling times. After 24 hours, the Y concentration was started to decline in a time-dependent manner at 48 and 72 hours. This indicated that as the days passed the concentration of particles was diluted. In contrast, MP-treated rats did not exhibit significant Y accumulation in any tissue and whole blood at any of the dose and time intervals. The amount of Y excreted in urine was significant at all doses of Y_2O_3 NPs at all sampling times in a dose- and time-dependent order, unlike the Y_2O_3 MP-treated group where there was no significant removal of Y. In feces, the Y content from both Y_2O_3 NPs and MPs was excreted significantly and the clearance was rapidly reduced from 24 to 72 hours. In contrast, with MP-treated rats more significant excretion of Y content in the feces was observed when compared to NP-treated rats.

4 | DISCUSSION

The Y_2O_3 NPs are considered as one of the most interesting NPs because of their several applications. Thus, the aim of this study was to evaluate the genotoxicity of Y_2O_3 NPs and compare it with their MPs after acute oral administration to albino female Wistar rats. To study the toxicity induced by engineered NPs, characterization of the NMs is mandatory. Moreover, the physicochemical properties could have an influence on the behavior of the particles and hence have an impact on toxicity. Further, appropriate quantitative analytical methods are essential to gather veritable data on NP properties (López-Heras, Madrid, & Cámara, 2014). Hence, TEM, DLS and LDV measurements were used to characterize the particles. The results obtained from the acute oral toxicity study have revealed that NP-induced toxic effects at high dose without any severe distress symptoms and mortality. In contrast, MPs have not shown toxicity at all test concentrations and at all sampling periods.

The doses ranged from highly toxic to least or no toxicity. The highest dose (1000 mg kg^{-1} bw) was selected to produce signs or some indications of toxicity when large quantities of NPs get released accidentally into the environment, and then enters the human body. Similar high doses were used to study the toxicity of CeO_2 and MnO_2 NPs (Kumari et al., 2014; Singh et al., 2013). However, the low dose of 250 mg kg^{-1} bw is likely intended to reflect human exposure, when workers get exposed to the NPs occupationally during the process of manufacturing unintentionally.

Genotoxicity is one of the essential parameters to evaluate the adverse effects of NPs along with the detection of mutations and cancer genetics. Comet assay showed that Y_2O_3 NPs could induce a significant increment in percentage tail DNA in PBL and liver cells in comparison to controls at 24- and 48-hour sampling times at 1000 mg kg^{-1} bw. The gradual reduction in the percentage tail DNA with time may be due to the action of complex DNA repair following removal of the DNA damaging agent (Karlsson, 2010). Similar results

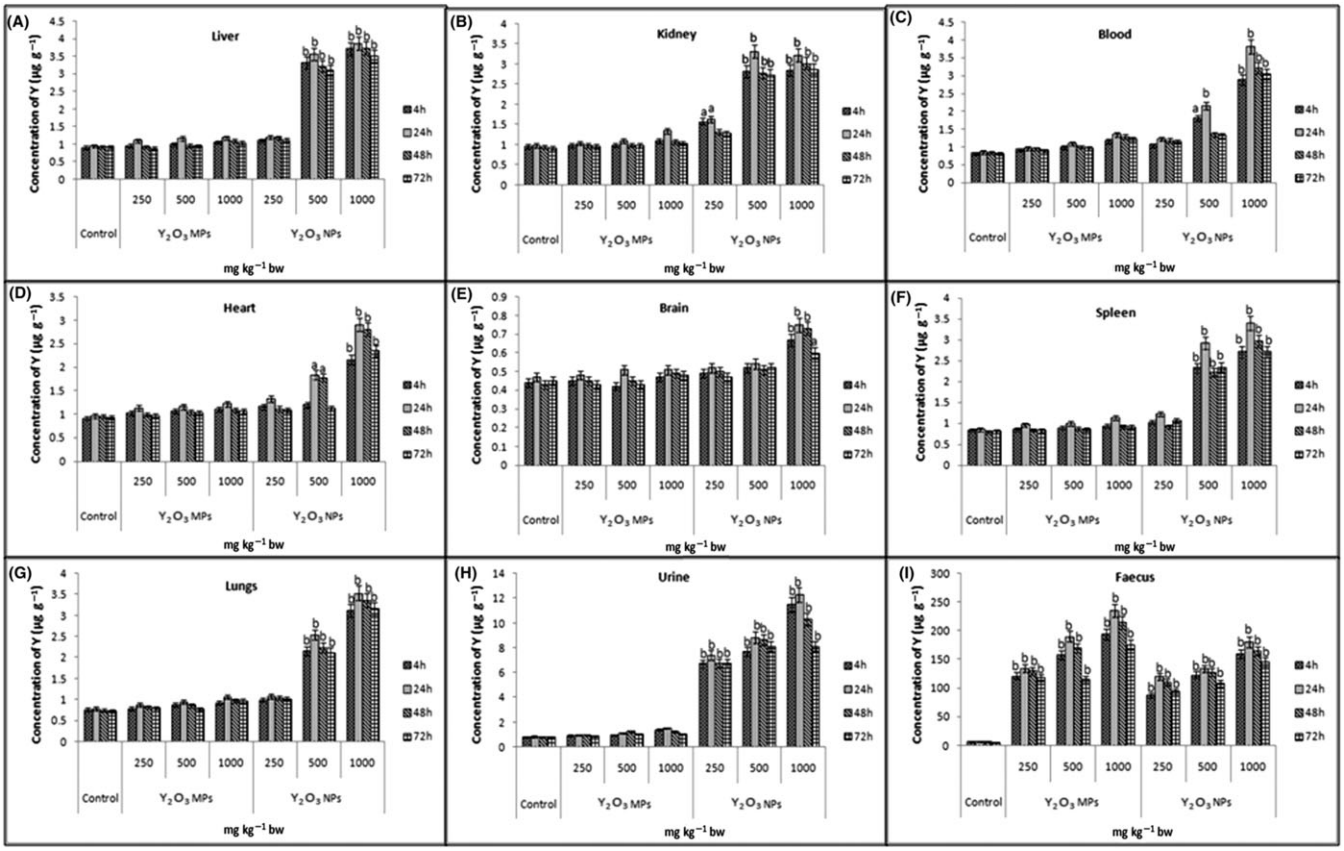

FIGURE 12 Tissue distribution of Y measured by inductively coupled plasma optical emission spectrometry in (A) liver, (B) kidneys, (C) blood, (D) brain, (E) heart, (F) spleen, (G) lungs, (H) urine and (I) feces of rats after 4, 24, 48 and 72 hours of single oral treatment with 1000, 500 and 250 mg kg^{-1} bw of Y_2O_3 NPs and Y_2O_3 MPs. Letters indicate a significant difference ($^aP < 0.01$, $^bP < 0.001$) with respect to control, $n = 5$ animals per group. MPs, microparticles; NPs, nanoparticles; Y, yttrium.

were observed with WO_3 NP-induced significant DNA damage via comet assay in rats exposed to 1000 mg kg^{-1} bw dose at 24 and 48 hours post-treatment in PBL and liver cells (Chinde et al., 2017). The bone marrow and PB MNT results revealed a significant increase in MN frequency at 1000 mg kg^{-1} bw dose of Y_2O_3 NPs at 24- and 48-hour sampling times. The results of the MNT showed the involvement of either clastogenic or aneugenic events. This impairment in cell cycle progression may be associated with NP toxicity. The percentage PCEs calculated in the Y_2O_3 NP-treated groups did not show any significant change in comparison to the control group, indicating that cell death had not occurred in any of the NP-treated groups in any time periods. Reports on other in vivo studies with Y_2O_3 NPs are not available. However, in support of our results, there are some in vitro studies with Y_2O_3 NPs. HEK 293 cells were utilized to investigate cytotoxicity caused by Y_2O_3 NPs with various cytotoxicity, genotoxicity and apoptosis assays. Exposure to Y_2O_3 NPs (12.25–50 μg ml^{-1}) was associated with DNA damage at 24 and 48 hours. Further, micronuclei formation was increased, following cellular incubation with 6.125 or 12.25 μg ml^{-1} Y_2O_3 NPs. The authors suggested that it is likely that oxidative stress functions as a mediator for Y_2O_3 NP-induced DNA damage (Selvaraj et al., 2014).

Serum enzyme aminotransferases analyses have become a standard measure of hepatotoxicity. In the present study, treatment of rats with Y_2O_3 NPs and MPs resulted in an increased enzymatic activity in serum, liver and decreased in kidney. However, significant increases were observed at 24 and 72 hours after treatment with 1000 mg kg^{-1} bw of Y_2O_3 NPs. Similar increased enzyme levels of AST and ALT in liver, serum and decreased enzyme levels of AST and ALT in kidney were found in Fe_2O_3 NP-treated rats after acute oral exposure (Kumari et al., 2013). Similar significantly increased levels of serum AST and ALT was found in TiO_2 NP-treated mice (Chen, Dong, Zhao, & Tang, 2009). Significantly higher levels of serum ALT levels in mice treated with TiO_2 NPs also reported (Liu et al., 2009). Significant enhancement in levels of serum ALT was also reported in Zn NP-treated mice, indicating liver necrosis (Wang et al., 2008). A study showed that serum level of AST increased significantly 24 hours after the Fe_2O_3 NP formulation injection in male Sprague–Dawley rats; however, there was slight transient increase in the serum ALT level (Jain et al., 2008). In the present study, treatment of rats with Y_2O_3 NPs and MPs resulted in an increased ALP levels in serum, liver and kidney. However, significant increases were observed at 24 and 72 hours after treatment with 1000 mg kg^{-1} bw of Y_2O_3 NPs. Oral exposure of rats to Ag NPs at various concentrations altered the serum and tissue levels of ALP relative to the control (Adeyemi & Adewumi, 2014). ALP showed a significant increase in mice treated with 150 and 300 μg g^{-1} Fe_3O_4 NPs, compared to unexposed controls (Parivar, Fard, Bayat, Alavian, & Motavaf, 2016).

Oxidative stress is said to be the main mechanism of NP toxicity (Hsin et al., 2008; Reeves, Davies, Dodd, & Jha, 2008; Xia et al., 2006). In this study, we have tried to determine the role of oxidative stress in treated rats, as oxidative stress is considered an important mechanism

in carcinogenesis (De Berardis et al., 2010). LPO can be defined as the oxidative deterioration of cell membrane lipids and has been used extensively as a marker of oxidative stress (Sayeed et al., 2003). The present study revealed that the MDA levels were significantly elevated in Y_2O_3 NP-treated rats at 24- and 72-hour sampling times at 1000 mg kg^{-1} bw in the serum, liver and kidneys suggesting that NPs might have induced free radical generation that further initiated MDA. Glutathione plays an important role in antioxidant defense, nutrient metabolism and regulation of cellular events and its deficiency contributes to oxidative stress, which plays a key role in aging and the pathogenesis of many diseases (Townsend, Tew, & Tapiero, 2003). GSH effectively scavenges free radicals and other ROS (e.g. hydroxyl radical, lipid peroxyl radical, peroxynitrite and H_2O_2) directly and indirectly through enzymatic reactions (Fang, Yang, & Wu, 2002). After the Y_2O_3 NP treatment, the GSH levels were decreased at the 24- and 72-hour sampling times at 1000 mg kg^{-1} bw in the serum, liver and kidneys possibly owing to increased utilization of GSH in neutralizing the free radicals generated. Probably, the levels of MDA may rise and GSH levels might decline when excessive ROS are produced signifying that the treated rats suffered an oxidative stress condition. The endogenous antioxidant system of comprising SOD and CAT play important roles in free radical and peroxide metabolism and is responsible in part for protecting the cells against oxidant stress (Wang et al., 2006). In antioxidant enzymes, SOD is always considered as the first line of defense against oxygen toxicity owing to its inhibitory effects on oxygen radical formation (Li, Li, & Randak, 2010). In this study, Y_2O_3 NPs strongly inhibited the SOD activity at the 24- and 72-hour sampling times at 1000 mg kg^{-1} bw in serum, liver and kidney. Similarly, SOD activity was inhibited due to the high flux of superoxide radicals resulting in H_2O_2 increase in cells (Li et al., 2010). CAT activity was increased in our study suggesting that Y_2O_3 NPs resulted in high levels of H_2O_2 production at the 24- and 72-hour sampling times at 1000 mg kg^{-1} bw in the serum, liver and kidneys (Powers & Jackson, 2008). LDH leakage is evidence for the penetration of NPs into cells and cell membrane damage (Balduzzi, Diociaiuti, De Berardis, Paradisi, & Paoletti, 2004; Wang et al., 2011). It has been well documented that LDH levels in the cell medium evaluated after the cells exposed to NPs (Ahamed, 2011; Akhtar et al., 2010; Hussain, Hess, Gearhart, Geiss, & Schlager, 2005). Enhancement in the LDH levels in the serum, liver and kidneys after Y_2O_3 NP exposure at the 24- and 72-hour sampling times at 1000 mg kg^{-1} bw indicating there might be injuries to the tissues in contrast to observations in the Y_2O_3 MP and control-treated groups. NMs interact with proteins and enzymes and interfere with the antioxidant defense mechanism, leading to ROS generation and subsequent apoptosis and necrosis (Schrand et al., 2010). From the current study, it was also noted that Y_2O_3 NP toxicity was mainly mediated through the altered antioxidant status of the cells.

In the present study, a significant biodistribution of Y_2O_3 NPs occurred in different tissues of treated rats. Our data revealed that maximum accumulation was in the liver followed by kidneys, heart, spleen, lungs and blood. This could be attributed to "Y" ions being entrapped in the reticuloendothelial system and excreted by the kidneys in treated rats. The levels of Y in urine from the Y_2O_3 NP-treated group showed a significant increase when compared to the control group. Y_2O_3 MP-treated rats showed extremely high levels of Y in the feces. Similar results were observed with Cu NPs. The study revealed that maximum accumulation of Cu was in the liver and kidneys of Cu NP-treated mice, whereas Cu MPs did not elevate Cu levels in the liver and kidney after a single acute oral treatment. The levels of Cu in urine and feces from the Cu NP-treated group showed a significant increase when compared to the control group. Cu MP-treated rats showed extremely high levels of Cu in the feces (Lee et al., 2016). Likewise, CeO_2 NPs were significantly distributed and destined to the liver, spleen, kidneys, heart and brain thus providing evidence that they could be transported to other sites subsequent to exposure due to their translocation into the blood. The most avid uptake and retention of NPs was detected in the liver, kidneys and spleen. The distribution was in a dose- and time-dependent order, as the amount absorbed increased the higher the dose administered (Kumari et al., 2014). It can be summarized that characteristics of NPs could have an influence on the toxicokinetic properties of the particles. Moreover, adverse effects of nano Y may be closely linked with the size-associated capacity to enter in the biological system without any difficulty. However, it is still unclear the extent that different NP characteristics contribute to their kinetics. As can be inferred from our results, the in vivo toxicity was directly connected to the biodistribution and bioaccumulation times, and both were particle size-dependent.

5 | CONCLUSION

In conclusion, results of the present study associated the size, dose and time of bioaccumulation of the Y_2O_3 NPs for its toxicity. To some extent, the low toxicity of Y_2O_3 NPs was perceived through the acute oral exposure, whereas Y_2O_3 MPs did not provoke any toxicity ascribed in comparison to controls. The results obtained in the present study indicated that Y_2O_3 NP-induced genotoxicity as well as biochemical changes only at the higher dose of 1000 mg kg^{-1} bw. From our results, it could be concluded that after acute oral administration of Y_2O_3 NPs and MPs, the accumulation was dose and time dependent. The dynamics of Y concentration in different tissues, urine and feces changed with time and the biodistribution and clearance profile of NPs showed concurrently composite events. Moreover, bioaccumulation of Y_2O_3 NPs was more marked in comparison to Y_2O_3 MPs. This indicates that the accumulated Y may have led to significant genotoxicological effects. It was also observed that Y_2O_3 NP toxicity could be mediated through the modified antioxidant status of the cells. Despite the fact that the absolute potentiality of NP toxicity is still ahead, however, the feasible mechanism might be either by ROS generated by the NPs or the NPs themselves. The present data add to the information of Y_2O_3 NPs to be able to interpret its toxicological implication. However, more studies are warranted for careful assessment to ensure the safety of Y_2O_3 NPs in biomedical applications.

ACKNOWLEDGEMENTS

We express our sincere thanks to the Director, IICT, Hyderabad, for providing funds and facilities to execute this study. Further, Archana Panyala (SRF), Paramjit Grover (Emeritus scientist) and Srinivas Chinde (SRF) are grateful to Council of Scientific and Industrial Research and Indian Council of Medical Research, India respectively for the award of fellowships.

CONFLICT OF INTEREST

There is no conflict of interest related to this research.

REFERENCES

Adeyemi, O. S., & Adewumi, I. (2014). Biochemical evaluation of silver nanoparticles in Wistar rats. *International Scholarly Research Notices*, 2014, 196091.

Aebi, H. (1984). Catalase in vitro. *Methods in Enzymology*, 105, 121–126.

Ahamed, M. (2011). Toxic response of nickel nanoparticles in human lung epithelial A549 cells. *Toxicology In Vitro*, 25, 930–936.

Akhtar, M. J., Ahamed, M., Kumar, S., Siddiqui, H., Patil, G., Ashquin, M., & Ahmad, I. (2010). Nanotoxicity of pure silica mediated through oxidant generation rather than glutathione depletion in human lung epithelial cells. *Toxicology*, 276, 95–102.

Andelman, T., Gordonov, S., Busto, G., Moghe, P. V., & Riman, R. E. (2010). Synthesis and cytotoxicity of Y2O3 nanoparticles of various morphologies. *Nanoscale Research Letters*, 5, 263.

Arooj, S., Nazir, S., Nadhman, A., Ahmad, N., Muhammad, B., Ahmad, I., … Abbasi, R. (2015). Novel ZnO: Ag nanocomposites induce significant oxidative stress in human fibroblast malignant melanoma (Ht144) cells. *Beilstein Journal of Nanotechnology*, 6, 570–582.

Balduzzi, M., Diociaiuti, M., De Berardis, B., Paradisi, S., & Paoletti, L. (2004). In vitro effects on macrophages induced by noncytotoxic doses of silica particles possibly relevant to ambient exposure. *Environmental Research*, 96, 62–71.

Biswas, P., & Wu, C.-Y. (2005). Nanoparticles and the environment. *Journal of the Air & Waste Management Association*, 55, 708–746.

Bour, G., Reinholdt, A., Stepanov, A., Keutgen, C., & Kreibig, U. (2001). Optical and electrical properties of hydrogenated yttrium nanoparticles. *European Physical Journal D – Atomic, Molecular, Optical and Plasma Physics*, 16, 219–223.

Castro-Bugallo, A., González-Fernández, Á., Guisande, C., & Barreiro, A. (2014). Comparative responses to metal oxide nanoparticles in marine phytoplankton. *Archives of Environmental Contamination and Toxicology*, 67, 483–493.

Çelik, A., Öğenler, O., & Çömelekoğlu, Ü. (2005). The evaluation of micronucleus frequency by acridine orange fluorescent staining in peripheral blood of rats treated with lead acetate. *Mutagenesis*, 20, 411–415.

Chen, J., Dong, X., Zhao, J., & Tang, G. (2009). In vivo acute toxicity of titanium dioxide nanoparticles to mice after intraperitioneal injection. *Journal of Applied Toxicology*, 29, 330–337.

Chinde, S., Dumala, N., Rahman, M. F., Kamal, S. S. K., Kumari, S. I., Mahboob, M., & Grover, P. (2017). Toxicological assessment of tungsten oxide nanoparticles in rats after acute oral exposure. *Environmental Science and Pollution Research*, 24, 13576–13593.

Chow, J. C., Watson, J. G., Savage, N., Solomon, C. J., Cheng, Y.-S., McMurry, P. H., … Pleus, R. C. (2005). Nanoparticles and the environment. *Journal of the Air & Waste Management Association*, 55, 1411–1417.

De Berardis, B., Civitelli, G., Condello, M., Lista, P., Pozzi, R., Arancia, G., & Meschini, S. (2010). Exposure to ZnO nanoparticles induces oxidative stress and cytotoxicity in human colon carcinoma cells. *Toxicology and Applied Pharmacology*, 246, 116–127.

Drobne, D. (2007). Nanotoxicology for safe and sustainable nanotechnology. *Arhiv za Higijenu Rada i Toksikologiju*, 58, 471–478.

Fang, Y.-Z., Yang, S., & Wu, G. (2002). Free radicals, antioxidants, and nutrition. *Nutrition*, 18, 872–879.

Fischer, H. C., & Chan, W. C. (2007). Nanotoxicity, the growing need for in vivo study. *Current Opinion in Biotechnology*, 18, 565–571.

Gojova, A., Guo, B., Kota, R. S., Rutledge, J. C., Kennedy, I. M., & Barakat, A. I. (2007). Induction of inflammation in vascular endothelial cells by metal oxide nanoparticles, effect of particle composition. *Environmental Health Perspectives*, 115, 403–409.

Gómez, M., Sánchez, D. J., Llobet, J. M., Corbella, J., & Domingo, J. (1997). The effect of age on aluminum retention in rats. *Toxicology*, 116, 1–8.

Hsin, Y.-H., Chen, C.-F., Huang, S., Shih, T.-S., Lai, P.-S., & Chueh, P. J. (2008). The apoptotic effect of nanosilver is mediated by a ROS- and JNK-dependent mechanism involving the mitochondrial pathway in NIH3T3 cells. *Toxicology Letters*, 179, 130–139.

Hussain, S., Hess, K., Gearhart, J., Geiss, K., & Schlager, J. (2005). In vitro toxicity of nanoparticles in BRL 3A rat liver cells. *Toxicology In Vitro*, 19, 975–983.

Jain, T. K., Reddy, M. K., Morales, M. A., Leslie-Pelecky, D. L., & Labhasetwar, V. (2008). Biodistribution, clearance, and biocompatibility of iron oxide magnetic nanoparticles in rats. *Molecular Pharmaceutics*, 5, 316–327.

Jollow, D., Mitchell, J., Zampaglione, N., & Gillette, J. (1974). Bromobenzene-induced liver necrosis. Protective role of glutathione and evidence for 3,4-bromobenzene oxide as the hepatotoxic metabolite. *Pharmacology*, 11, 151–169.

Kannan, S., & Sundrarajan, M. (2015). Biosynthesis of yttrium oxide nanoparticles using *Acalypha indica* leaf extract. *Bulletin of Materials Science*, 38, 945–950.

Karlsson, H. L. (2010). The comet assay in nanotoxicology research. *Analytical and Bioanalytical Chemistry*, 398, 651–666.

Kumari, M., Kumari, S. I., Kamal, S. S. K., & Grover, P. (2014). Genotoxicity assessment of cerium oxide nanoparticles in female Wistar rats after acute oral exposure. *Mutation Research: Genetic Toxicology and Environmental Mutagenesis*, 775, 7–19.

Kumari, M., Rajak, S., Singh, S. P., Murty, U. S., Mahboob, M., Grover, P., & Rahman, M. F. (2013). Biochemical alterations induced by acute oral doses of iron oxide nanoparticles in Wistar rats. *Drug and Chemical Toxicology*, 36, 296–305.

Kuppusamy, P., Yusoff, M. M., Maniam, G. P., & Govindan, N. (2016). Biosynthesis of metallic nanoparticles using plant derivatives and their new avenues in pharmacological applications – An updated report. *Saudi Pharmaceutical Journal*, 24, 473–484.

Lee, I.-C., Ko, J.-W., Park, S.-H., Shin, N.-R., Shin, I.-S., Moon, C., … Kim, J.-C. (2016). Comparative toxicity and biodistribution assessments in rats following subchronic oral exposure to copper nanoparticles and microparticles. *Particle and Fibre Toxicology*, 13, 56.

Li, Z. H., Li, P., & Randak, T. (2010). Effect of a human pharmaceutical carbamazepine on antioxidant responses in brain of a model teleost in vitro, an efficient approach to biomonitoring. *Journal of Applied Toxicology*, 30, 644–648.

Liu, H., Ma, L., Zhao, J., Liu, J., Yan, J., Ruan, J., & Hong, F. (2009). Biochemical toxicity of nano-anatase TiO2 particles in mice. *Biological Trace Element Research*, 129, 170–180.

López-Heras, I., Madrid, Y., & Cámara, C. (2014). Prospects and difficulties in TiO2 nanoparticles analysis in cosmetic and food products using asymmetrical flow field-flow fractionation hyphenated to inductively coupled plasma mass spectrometry. *Talanta*, 124, 71–78.

Lowry, O. H., Rosebrough, N. J., Farr, A. L., & Randall, R. J. (1951). Protein measurement with the Folin phenol reagent. *Journal of Biological Chemistry*, 193, 265–275.

Marklund, S., & Marklund, G. (1974). Involvement of the superoxide anion radical in the autoxidation of pyrogallol and a convenient assay for superoxide dismutase. *European Journal of Biochemistry*, 47, 469–474.

McQueen, M. (1972). Optimal assay of LDH and α-HBD at 37°C. *Annals of Clinical Biochemistry*, 9, 21–25.

Montanari, S., & Gatti, A. M. (2016). *Nanopathology, The health impact of nanoparticles*CRC Press.

Murdock, R. C., Braydich-Stolle, L., Schrand, A. M., Schlager, J. J., & Hussain, S. M. (2008). Characterization of nanomaterial dispersion in solution prior to in vitro exposure using dynamic light scattering technique. *Toxicological Sciences*, 101, 239–253.

Negahdary, M., Chelongar, R., Zadeh, S. K., & Ajdary, M. (2015). The antioxidant effects of silver, gold, and zinc oxide nanoparticles on male mice in in vivo condition. *Advanced Biomedical Research*, 4, 69.

OECD. (2001). 420, acute oral toxicity-fixed dose procedure. *OECD Guidelines for Testing of Chemicals. Section*, 4, 1–14.

OECD. (2014). Test No. In *474*, *Mammalian Erythrocyte Micronucleus Test*. OecD: Publishing.

Oberdörster, G., Stone, V., & Donaldson, K. (2007). Toxicology of nanoparticles, a historical perspective. *Nanotoxicology*, 1, 2–25.

Parivar, K., Fard, F. M., Bayat, M., Alavian, S. M., & Motavaf, M. (2016). Evaluation of iron oxide nanoparticles toxicity on liver cells of BALB/c rats. *Iranian Red Crescent Medical Journal*, 18. e28939

Park, E.-J., & Park, K. (2009). Oxidative stress and pro-inflammatory responses induced by silica nanoparticles in vivo and in vitro. *Toxicology Letters*, 184, 18–25.

Powers, S. K., & Jackson, M. J. (2008). Exercise-induced oxidative stress, cellular mechanisms and impact on muscle force production. *Physiological Reviews*, 88, 1243–1276.

Prabhakar, P., Reddy, U. A., Singh, S., Balasubramanyam, A., Rahman, M., Indu Kumari, S., … Mahboob, M. (2012). Oxidative stress induced by aluminum oxide nanomaterials after acute oral treatment in Wistar rats. *Journal of Applied Toxicology*, 32, 436–445.

Reeves, J. F., Davies, S. J., Dodd, N. J., & Jha, A. N. (2008). Hydroxyl radicals (OH) are associated with titanium dioxide (TiO2) nanoparticle-induced cytotoxicity and oxidative DNA damage in fish cells. *Mutation Research: Fundamental and Molecular Mechanisms of Mutagenesis*, 640, 113–122.

Sayeed, I., Parvez, S., Pandey, S., Bin-Hafeez, B., Haque, R., & Raisuddin, S. (2003). Oxidative stress biomarkers of exposure to deltamethrin in freshwater fish, *Channa punctatus* Bloch. *Ecotoxicology and Environmental Safety*, 56, 295–301.

Schrand, A. M., Rahman, M. F., Hussain, S. M., Schlager, J. J., Smith, D. A., & Syed, A. F. (2010). Metal-based nanoparticles and their toxicity assessment. *Wiley Interdisciplinary Reviews, Nanomedicine and Nanobiotechnology*, 2, 544–568.

Schubert, D., Dargusch, R., Raitano, J., & Chan, S.-W. (2006). Cerium and yttrium oxide nanoparticles are neuroprotective. *Biochemical and Biophysical Research Communications*, 342, 86–91.

Selvaraj, V., Bodapati, S., Murray, E., Rice, K. M., Winston, N., Shokuhfar, T., … Blough, E. (2014). Cytotoxicity and genotoxicity caused by yttrium oxide nanoparticles in HEK293 cells. *International Journal of Nanomedicine*, 9, 1379–1391.

Singh, S. P., Kumari, M., Kumari, S. I., Rahman, M. F., Kamal, S. K., Mahboob, M., & Grover, P. (2013). Genotoxicity of nano- and micron-sized manganese oxide in rats after acute oral treatment. *Mutation Research: Genetic Toxicology and Environmental Mutagenesis*, 754, 39–50.

Sönmez, E., Türkez, H., Aydın, E., Özgeriş, F. B., Öztetik, E., Kerli, S., … Stefano, A. D. (2015). Hepatic effects of yttrium oxide nanoflowers, in vitro risk evaluation. *Toxicological & Environmental Chemistry*, 97, 599–608.

Townsend, D. M., Tew, K. D., & Tapiero, H. (2003). The importance of glutathione in human disease. *Biomedicine & Pharmacotherapy*, 57, 145–155.

US Geological Survey (2015). Mineral commodity summaries 2015, US Geological Survey, p. 196. https://doi.org/10. 3133/70140094

Wang, B., Feng, W., Wang, M., Wang, T., Gu, Y., Zhu, M., … Zhao, Y. (2008). Acute toxicological impact of nano- and submicro-scaled zinc oxide powder on healthy adult mice. *Journal of Nanoparticle Research*, 10, 263–276.

Wang, F., Jiao, C., Liu, J., Yuan, H., Lan, M., & Gao, F. (2011). Oxidative mechanisms contribute to nanosize silican dioxide-induced developmental neurotoxicity in PC12 cells. *Toxicology In Vitro*, 25, 1548–1556.

Wang, J., Chen, C., Li, B., Yu, H., Zhao, Y., Sun, J., … Tang, J. (2006). Antioxidative function and biodistribution of [Gd@C82(OH)22]n nanoparticles in tumor-bearing mice. *Biochemical Pharmacology*, 71, 872–881.

Wills, E. (1969). Lipid peroxide formation in microsomes. Relationship of hydroxylation to lipid peroxide formation. *Biochemical Journal*, 113, 333–341.

Xia, T., Kovochich, M., Brant, J., Hotze, M., Sempf, J., Oberley, T., … Nel, A. E. (2006). Comparison of the abilities of ambient and manufactured nanoparticles to induce cellular toxicity according to an oxidative stress paradigm. *Nano Letters*, 6, 1794–1807.

Yatzidis, H. (1960). Measurement of transaminases in serum. *Nature*, 186, 79–80.

Zhou, G., Li, Y., Ma, Y., Liu, Z., Cao, L., Wang, D., … Wang, W. (2016). Size-dependent cytotoxicity of yttrium oxide nanoparticles on primary osteoblasts in vitro. *Journal of Nanoparticle Research*, 18, 1–14.

How to cite this article: Panyala A, Chinde S, Kumari SI, Grover P. Assessment of genotoxicity and biodistribution of nano- and micron-sized yttrium oxide in rats after acute oral treatment. *J Appl Toxicol*. 2017;37:1379–1395. https://doi.org/10.1002/jat.3505